Inorg. Chem. **2007**, *46*, 6382–6394

Reactivity Studies on Fe^{III}–(O_2^{2-})–Cu^{II} Compounds: Influence of the Ligand Architecture and Copper Ligand Denticity

Eduardo E. Chufán,[§] Biplab Mondal,[§] Thirumanavelan Gandhi,[§] Eunsuk Kim,[§] Nick D. Rubie,[‡] Pierre Moënne-Loccoz,[‡] and Kenneth D. Karlin*[,§]

Department of Chemistry, Johns Hopkins University, Baltimore, Maryland, Maryland 21218, and Department of Environmental & Biomolecular Systems, OGI School of Science & Engineering, Oregon Health & Science University, Beaverton, Oregon 97006

Received February 26, 2007

Heme–Cu/O_2 adducts are of interest in the elucidation of the fundamental metal–O_2 chemistry occurring in heme–Cu enzymes which effect reductive O–O cleavage of dioxygen to water. In this report, the chemistry of four heme–peroxo–copper [Fe^{III}–(O_2^{2-})–Cu^{II}]$^+$ complexes (**1**–**4**), varying in their ligand architecture, copper-ligand denticity, or both and thus their structures and physical properties are compared in their reactivity toward CO, PPh_3, acids, cobaltocene, and phenols. In **1** and **2**, the copper(II) ligand is N_4-tetradentate, and the peroxo unit is bound side-on to iron(III) and end-on to the copper(II). In contrast, **3** and **4** contain a N_3-tridentate copper(II) ligand, and the peroxo unit is bound side-on to both metal ions. CO "displaces" the peroxo ligand from **2**–**4** to form reduced CO–Fe^{II} and CO–Cu^{I} species. PPh_3 reacts with **3** and **4** displacing the peroxide ligand from copper, forming (porphyrinate)Fe^{III}-superoxide plus Cu^{I}-PPh_3 species. Complex **2** does not react with PPh_3, and surprisingly, **1** reacts neither with PPh_3 nor CO, exhibiting remarkable stability toward these reagents. The behavior of **1** and **2** compared to that of **3** and **4** correlates with the different denticity of the copper ligand (tetra vs tridentate). Complexes **1**–**4** react with HCl releasing H_2O_2, demonstrating the basic character of the peroxide ligand. Cobaltocene causes the two-electron reduction of **1**–**4** giving the corresponding μ-oxo [Fe^{III}–(O^{2-})–Cu^{II}]$^+$ complexes, in contrast to the findings for other heme-peroxo-copper species of different design. With *t*-butyl-substituted phenols, no reaction occurs with **1**–**4**. The results described here emphasize how ligand design and variations influence and control not only the structure and physical properties but also the reactivity patterns for heme–Cu/O_2 adducts. Implications for future investigations of protonated heme/Cu–peroxo complexes, low-spin analogues, and ultimately O–O cleavage chemistry are discussed.

Introduction

The chemistry at metalloprotein active sites cannot be disconnected from the inherent fundamental chemistry associated with the metal ion and its ligand environment.[1−3] Furthermore, the relationship between structure and reactivity for a given chemical system is part of the basic knowledge required to obtain a deep understanding of chemical function. In this report, we describe systematic studies concerning reactivity patterns for a series of heme−peroxo−copper complexes, Fe^{III}−(O_2^{2-})−Cu^{II}(ligand), which possess varying structures depending on the nature of the ligand on copper. Our interest in this series comes as part of our program whose goal is to elucidate the underlying chemistry occurring at the active site of heme−copper oxidases.[4−6] There has been an emphasis on dioxygen reactivity to unravel the chemistry of O_2 binding in the presence of both heme and copper complexes, given a previously established separate heme−O_2[7,8] and copper−O_2[9−11] chemistries.

* To whom correspondence should be addressed. E-mail: karlin@jhu.edu.
§ Johns Hopkins University.
‡ Oregon Health & Science University.

(1) Lee, Y.; Karlin, K. D. Highlights of Copper Protein Active-Site Structure/Reactivity and Synthetic Model Studies; In *Concepts and Models in Bioinorganic Chemistry*; Metzler-Nolte, N., Kraatz, H.-B., Eds.; Wiley-VCH: New York, 2006; pp 363−395.
(2) Karlin, K. D. *Science* **1993**, *261*, 701−708.
(3) Holm, R. H.; Solomon, E. I. *Chem. Rev.* **2004**, *104*, 347−348.
(4) Chufan, E. E.; Puiu, S. C.; Karlin, K. D. *Acc. Chem. Res.* **2007**, in press.
(5) Kim, E.; Chufán, E. E.; Kamaraj, K.; Karlin, K. D. *Chem. Rev.* **2004**, *104*, 1077−1133.
(6) Collman, J. P.; Boulatov, R.; Sunderland, C. J.; Fu, L. *Chem. Rev.* **2004**, *104*, 561−588.
(7) Momenteau, M.; Reed, C. A. *Chem. Rev.* **1994**, *94*, 659−698.

10.1021/ic700363k CCC: $37.00
Published on Web 07/06/2007

Chart 1

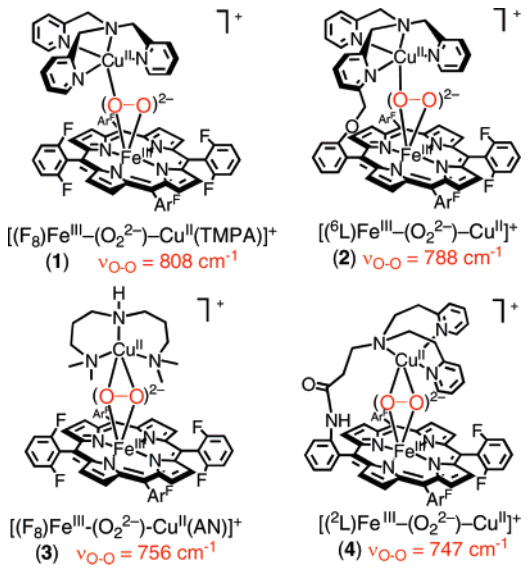

Heme−copper oxidases include cytochrome *c* oxidase (C*c*O), which is the terminal enzyme of the respiratory chain of mitochondria and many aerobic bacteria. It catalyzes the reduction of molecular oxygen to water, a process that requires four electrons and four protons. The reaction is coupled to the pumping of four additional protons across the mitochondrial or bacterial membrane.[5,12] In the mechanism of O_2-reduction by C*c*O, a key step is the O−O reductive cleavage of the bound dioxygen moiety.[13] A well-established early enzyme intermediate is a Fe^{III}−(O$_2^{-}$)···Cu^{I} species (**A**); however, a transient peroxo complex, formally Fe^{III}−(O$_2^{2-}$)···Cu^{II}, possibly bridged between the two metals, is often considered to form subsequently.[14−16]

By reaction of O_2 with either a 1:1 mixture of reduced hemes (i.e., Fe^{II}) and copper(I) complexes or with Fe^{II}···Cu^{I} complexes employing binucleating ligands (i.e., a porphyrin with appended/tethered tridentate or tetradentate ligand for copper), a series of (porphyrinate)Fe^{III}-(O$_2^{2-}$)-Cu^{II}(ligand) complexes have been generated and characterized; they all possess a high-spin iron(III) ion (Chart 1).[4,17] In [(F$_8$)Fe^{III}-(O$_2^{2-}$)-Cu^{II}(TMPA)]$^+$ (**1**) {F$_8$ = tetrakis(2,6-difluorophenyl)-porphyrinate}, the copper ion is coordinated by a tripodal tetradentate tris(2-pyridylmethyl)amine (TMPA).[18] The Fe···Cu distance is 3.7 Å (EXAFS determination).[19] The peroxo unit is bound side-on to the high-spin iron(III) (thus overall five-coordinate with the iron out of the porphryinate plane) and end-on to the copper(II), thus in an overall μ-η^2:η^1 coordination mode,[19] ν_{O-O} = 808 cm^{-1} (resonance Raman spectroscopy).[18] This complex is structurally analogous to that synthesized and crystallographically characterized by Naruta and co-workers.[20] In [(6L)Fe^{III}-(O$_2^{2-}$)-Cu^{II}]$^+$ (**2**), the tetradentate TMPA ligand is covalently appended to the periphery of a 2,6-difluorophenyl-substituted porphyrin and ν_{O-O} = 788 cm^{-1}.[21,22] A second group of complexes are rather different in aspects of their physical properties. In [(F$_8$)Fe^{III}-(O$_2^{2-}$)-Cu^{II}(AN)]$^+$ (**3**) {AN = 3,3′-iminobis(*N*,*N*-dimethyl-propylamine} (vide infra) and [(2L)Fe^{III}-(O$_2^{2-}$)-Cu^{II}]$^+$ (**4**)[23,24] (Chart 1), the copper(II) ion is coordinated by a tridentate ligand; the difference between the two is that the latter possesses a linker between the heme and copper chelate, see Chart 1. This different environment for copper in both of these complexes, compared to that of **1** and **2**, is reflected in the O−O stretching frequency which is considerably lowered: ν_{O-O} for **3** is 756 cm^{-1} (vide infra) and that for **4** is 747 cm^{-1}.[23,24] This lower ν_{O-O} reflects a different mode of coordination, side-on bound to both iron and copper ions, thus in an overall μ-η^2:η^2-peroxo ligation.[4,24,25]

Probing the reactivity of a complex or series of compounds by subjecting them to a series of reagents is one good way to elucidate structure−reactivity (functional) relationships. Such approaches and systematic investigations have been carried out with O_2-derived complexes, for example "classical" M−peroxo complexes (M = Pt, Rh, ...),[26] copper−dioxygen complexes (as μ-peroxo-dicopper(II) species), which turn out to either have a nucleophilic or electrophilic character (depending on the ligand),[27,28] η^2-peroxo-iron(III)

(8) Traylor, T. G.; Traylor, P. S. Reaction of Dioxygen and Its Reduced Forms with Heme Proteins and Model Porphyrin Complexes. In *Active Oxygen: Active Oxygen in Biochemistry*; Valentine, J. S., Foote, C. S., Greenberg, A., Liebman, J. F., Eds.; Chapman & Hall: New York, 1995; pp 84−187.
(9) Quant Hatcher, L.; Karlin, K. D. *J. Biol. Inorg. Chem.* **2004**, *9*, 669−683.
(10) Lewis, E. A.; Tolman, W. B. *Chem. Rev.* **2004**, *104*, 1047−1076.
(11) Mirica, L. M.; Ottenwaelder, X.; Stack, T. D. P. *Chem. Rev.* **2004**, *104*, 1013−1045.
(12) Ferguson-Miller, S.; Babcock, G. T. *Chem. Rev.* **1996**, *96*, 2889−2907.
(13) Ogura, T.; Kitagawa, T. *Biochim. Biophys. Acta* **2004**, *1655*, 290−297.
(14) Proshlyakov, D. A.; Pressler, M. A.; Babcock, G. T. *Proc. Natl. Acad. Sci. U.S.A.* **1998**, *95*, 8020−8025.
(15) Blomberg, M. R. A.; Siegbahn, P. E. M.; Wikström, M. *Inorg. Chem.* **2003**, *42*, 5231−5243.
(16) Blomberg, M. R. A.; Siegbahn, P. E. M. *Biochim. Biophys. Acta* **2006**, *1757*, 969−980.
(17) Ghiladi, R. A.; Chufan, E. E.; del Rio, D.; Solomon, E. I.; Krebs, C.; Huynh, B. H.; Huang, H.-w.; Moenne-Loccoz, P.; Kaderli, S.; Honecker, M.; Zuberbuhler, A. D.; Marzilli, L.; Cotter, R. J.; Karlin, K. D. *Inorg. Chem.* **2007**, *46*, 3889−3902.
(18) Ghiladi, R. A.; Hatwell, K. R.; Karlin, K. D.; Huang, H.-w.; Moënne-Loccoz, P.; Krebs, C.; Huynh, B. H.; Marzilli, L. A.; Cotter, R. J.; Kaderli, S.; Zuberbühler, A. D. *J. Am. Chem. Soc.* **2001**, *123*, 6183−6184.
(19) del Rio, D.; Sarangi, R.; Chufán, E. E.; Karlin, K. D.; Hedman, B.; Hodgson, K. O.; Solomon, E. I. *J. Am. Chem. Soc.* **2005**, *127*, 11969−11978.
(20) Chishiro, T.; Shimazaki, Y.; Tani, F.; Tachi, Y.; Naruta, Y.; Karasawa, S.; Hayami, S.; Maeda, Y. *Angew. Chem., Int. Ed.* **2003**, *42*, 2788−2791.
(21) Ghiladi, R. A.; Huang, H. W.; Moënne-Loccoz, P.; Stasser, J.; Blackburn, N. J.; Woods, A. S.; Cotter, R. J.; Incarvito, C. D.; Rheingold, A. L.; Karlin, K. D. *J. Biol. Inorg. Chem.* **2005**, *10*, 63−77.
(22) Ghiladi, R. A.; Ju, T. D.; Lee, D.-H.; Moënne-Loccoz, P.; Kaderli, S.; Neuhold, Y.-M.; Zuberbühler, A. D.; Woods, A. S.; Cotter, R. J.; Karlin, K. D. *J. Am. Chem. Soc.* **1999**, *121*, 9885−9886.
(23) Kim, E.; Helton, M. E.; Lu, S.; Moënne-Loccoz, P.; Incarvito, C. D.; Rheingold, A. L.; Kaderli, S.; Zuberbühler, A. D.; Karlin, K. D. *Inorg. Chem.* **2005**, *44*, 7014−7029.
(24) Kim, E.; Shearer, J.; Lu, S.; Moënne-Loccoz, P.; Helton, M. E.; Kaderli, S.; Zuberbühler, A. D.; Karlin, K. D. *J. Am. Chem. Soc.* **2004**, *126*, 12716−12717.
(25) Karlin, K. D.; Kim, E. *Chem. Lett.* **2004**, *33*, 1226−1231.
(26) Sheldon, R. A.; Kochi, J. K. *Metal-Catalyzed Oxidations of Organic Compounds*; Academic Press: New York, 1981.
(27) Hatcher, L. Q.; Karlin, K. D. *Adv. Inorg. Chem.* **2006**, *58*, 131−184.
(28) Paul, P. P.; Tyeklár, Z.; Jacobson, R. R.; Karlin, K. D. *J. Am. Chem. Soc.* **1991**, *113*, 5322−5332.

hemes,[29] and others.[30] In the discussion that follows, the four peroxo complexes, **1**−**4** (Chart 1), are compared in their reactivity toward five reagents: (i) carbon monoxide (CO), (ii) triphenylphosphine (PPh_3), (iii) HCl or other acids as proton sources, (iv) cobaltocene ($Co(Cp)_2$) as an electron donor, and (v) *t*-butyl-substituted phenols as potential proton/electron donors. The molecules CO and PPh_3 help to probe the environment of the heme−copper assembly, possibly displacing the peroxide, perhaps as CO displaces O_2 (bound as superoxide) in oxy-hemoglobin or oxy-myoglobin to regenerate the reduced (Fe^{II}) enzyme.[6,31] PPh_3 may also cause a displacement or possibly be oxygenated. Protonation of reductively cleaved O_2-derived species is obviously of importance in C*c*O chemistry whose function is not only "dioxygen activation" but also proton translocation;[32] thus, determination of the reactivity of protons with complexes **1**−**4** is of interest. Because the enzymatic reduction of O_2 (to water) requires 2 more electrons to go beyond the peroxo stage found in complexes **1**−**4**, the addition of cobaltocene was deemed to be of interest for study. Further, $Co(Cp)_2$ has been used by Collman and co-workers[33−36] to chemically probe the overall oxidation state of heme−peroxo−copper complexes. Reactions of **1**−**4** with phenols complement such reduction chemistry.

Results and Discussion

Complex $[(F_8)Fe^{III}\text{-}(O_2^{2-})\text{-}Cu^{II}(AN)]^+$ (3). This heterobinuclear heme−peroxo−copper complex was employed in the present studies because it is easier and cheaper to generate than a previously well-studied system employing $[(F_8)Fe^{III}\text{-}(O_2^{2-})Cu^{II}(L^{Me_2N})]^+$,[37] where L^{Me_2N} is the tridentate donor ligand *N*,*N*-bis{2-[2-(*N*,*N*-4-dimethylamino)pyridyl]-ethyl}methylamine. However, **3** has not been previously described so we report its characteristics here. Peroxo complex **3** can be generated by bubbling O_2 at −80 °C through an equimolar solution of $(F_8)Fe^{II}$ and $[Cu^I(AN)](B(C_6F_5)_4)$ in THF, pre-placed in a Schlenk flask, cuvette assembly, or NMR tube in an inert atmosphere glove box (See Experimental Section). The UV−vis changes which occur during this reaction are given in Scheme 1, and the actual spectra are shown in Figure 1. Low-temperature ^1H

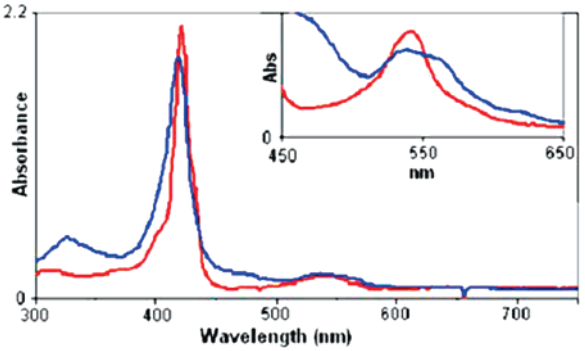

Figure 1. UV−vis spectra of reduced species, 1:1 mixture of $(F_8)Fe^{II}$ and $[Cu^I(AN)](B(C_6F_5)_4)$ (red trace, λ_{max} = 422, 542 nm), and of μ-peroxo complex $[(F_8)Fe^{III}\text{-}(O_2^{2-})\text{-}Cu^{II}(AN)]^+$ (**3**) (blue trace, λ_{max} = 418, 478, 538, 561 nm) in THF at −80 °C. The inset shows the α-region of the spectra.

Scheme 1

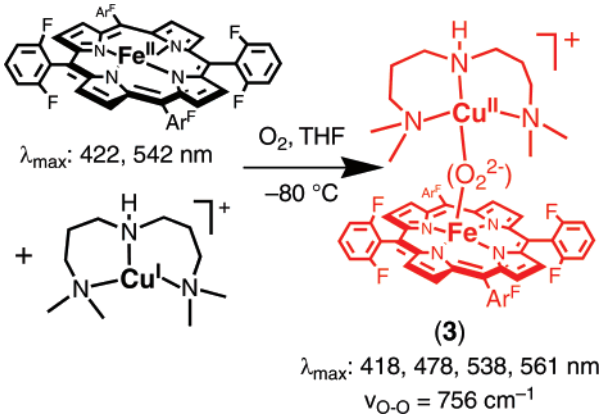

NMR characterization of the μ-peroxo product **3** shows a downfield-shifted pyrrole resonance at 96 ppm (spectrum not shown) with a small amount of the μ-oxo decompostion product $[(F_8)Fe^{III}\text{-O-}Cu^{II}(AN)]^+$. The persistent formation of 10−20% of μ-oxo species at NMR scale is not observed however at lower concentration (e.g., at Soret and Q-band UV−vis scale, where distinctive and readily seen changes from the peroxo complex occurs; see Supporting Information (Figures S1) for the μ-oxo UV−vis spectrum). The 96 ppm pyrrole chemical shift position found for peroxo complex **3** (and confirmed by ^2H NMR studies using the pyrrole-deuterated (d_8-F_8)Fe^{II} analogue) excludes the possibility that this complex is (i) the μ-peroxo complex $[(F_8)Fe^{III}]_2\text{−}(O_2^{2-})$ (17.5 ppm, −80 °C), (ii) an iron−superoxide, that is, $(F_8)\text{-}Fe^{III}\text{−}(O_2^{-})$ (8.9 ppm, −80 °C), (iii) the ferryl species $(F_8)\text{-}Fe^{IV}$=O (3.5 ppm, −80 °C), or (iv) $(F_8)Fe^{III}$−OH (∼135 ppm, −80 °C).[38] In fact, the 96 ppm pyrrole resonance in **3** is in the range expected for a high-spin Fe^{III} (d^5, S = 5/2) system which is strongly antiferromagnetically coupled to Cu^{II} ion (d^9, S = 1/2), giving an overall S = 2 spin system.[5] Further, resonance Raman spectroscopy (rR) (Figure 2) reveals a dominant peroxide O−O stretching vibration at 756 cm^{-1} ($\Delta^{18}O_2$ = −48 cm^{-1}). Another O−O vibration at 746 cm^{-1} ($\Delta^{18}O_2$ = −48 cm^{-1}) is observed as a shoulder to the major component at 756 cm^{-1} and probably represents a

(29) Selke, M.; Sisemore, M. F.; Valentine, J. S. *J. Am. Chem. Soc.* **1996**, *118*, 2008−2012.
(30) Groves, J. T.; Gross, Z.; Stern, M. K. *Inorg. Chem.* **1994**, *33*, 5065−5072.
(31) Walker, F. A.; Simonis, U. Iron Porphyrin Chemistry. In *Encyclopedia of Inorganic Chemistry*, 2nd ed.; King, R. B., Ed.; John Wiley & Sons Ltd.: New York, 2005; Vol. IV, pp 2390−2521.
(32) Wikstrom, M.; Verkhovsky, M. I. *Biochim. Biophys. Acta* **2006**, *1757*, 1047−1051.
(33) Collman, J. P.; Herrmann, P. C.; Boitrel, B.; Zhang, X.; Eberspacher, T. A.; Fu, L.; Wang, J.; Rousseau, D. L.; Williams, E. R. *J. Am. Chem. Soc.* **1994**, *116*, 9783−9784.
(34) Collman, J. P.; Fu, L.; Herrmann, P. C.; Zhang, X. *Science* **1997**, *275*, 949−951.
(35) Collman, J. P. *Inorg. Chem.* **1997**, *36*, 5145−5155.
(36) Collman, J. P.; Fu, L.; Herrmann, P. C.; Wang, Z.; Rapta, M.; Bröring, M.; Schwenninger, R.; Boitrel, B. *Angew. Chem., Int. Ed.* **1998**, *37*, 3397−3400.
(37) Kim, E.; Helton, M. E.; Wasser, I. M.; Karlin, K. D.; Lu, S.; Huang, H.-w.; Moënne-Loccoz, P.; Incarvito, C. D.; Rheingold, A. L.; Honecker, M.; Kaderli, S.; Zuberbühler, A. D. *Proc. Natl. Acad. Sci. U.S.A.* **2003**, *100*, 3623−3628.
(38) Ghiladi, R. A.; Kretzer, R. M.; Guzei, I.; Rheingold, A. L.; Neuhold, Y.-M.; Hatwell, K. R.; Zuberbühler, A. D.; Karlin, K. D. *Inorg. Chem.* **2001**, *40*, 5754−5767.

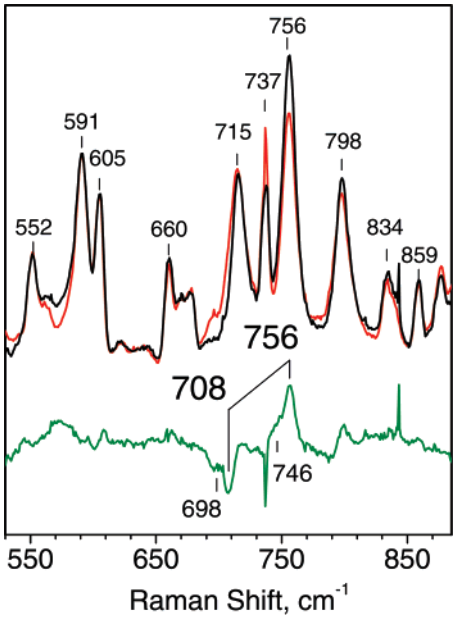

Figure 2. Resonance Raman spectra of [(F_8)Fe^{III}-(O_2^{2-})-Cu^{II}(AN)]$^+$ (**3**), formed by the oxygenation of an equimolar solution of (F_8)Fe^{II} and [Cu^{I}-(AN)]($B(C_6F_5)_4$) in THF with $^{16}O_2$ (black) and $^{18}O_2$ (red). The difference spectrum ($^{16}O_2$ minus $^{18}O_2$) is also shown (green). All spectra were obtained at 90 K with 413 nm excitation.

minor conformer of **3** where the Cu(AN) ligand moiety resides at a different orientation with respect to the peroxo O−O axis. This interpretation is consistent with our previous analysis of [(F_8)Fe^{III}-(O_2^{2-})Cu^{II}(L^{Me_2N})]$^+$, where two conformers were also detected by rR spectroscopy.[37] The minor component observed in the rR spectra of **3** appears to increase in intensity during the course of these experiments, suggesting that laser illumination might promote isomerization of the peroxo complex. Exposure of [Cu^{I}(AN)]$^+$ to O_2 in THF is known to form a mixture of μ-η^2:η^2-peroxo complex [{Cu^{II}(AN)}$_2$(O_2)]$^{2+}$ and bis-μ-oxo complex [{Cu^{III}(AN)}$_2$-(O_2)]$^{2+}$ with characteristic ν_{O-O} at 721 cm^{-1} (683 cm^{-1} for $^{18}O_2$) and ν_{Cu-O} at 608 cm^{-1} (580 cm^{-1} for $^{18}O_2$), respectively.[39] The 413 nm rR spectra provide no evidence for such species in the presence of (F_8)Fe^{II}, since the 413 nm excitation is expected to strongly favor porphyrin related vibrations at the expense of putative Cu-only complexes. This rR information about Cu-only complexes by itself cannot categorically rule these out; however, the single Soret band and pyrrole signal found for [(F_8)Fe^{III}-(O_2^{2-})-Cu^{II}(AN)]$^+$ precludes formation of the Cu-only Cu^{II}−(O_2^{2-})−Cu^{II} or bis-μ-oxo Cu^{III}−(O)$_2$−Cu^{III} species to the extent of 0−5% total. Following the spectroscopic analysis and arguments described previously for [(^{2}L)Fe^{III}-(O_2^{2-})-Cu^{II}]$^+$ (**4**) and [(F_8)-Fe^{III}-(O_2^{2-})Cu^{II}(L^{Me2N})]$^{+}$,[24,25] the relatively low ν(O−O) frequencies observed in **3** support a μ-η^2:η^2-peroxo ligation to both iron and copper, as shown in Chart 1.

General Approach and Conditions for Reactivity Studies. All Fe^{III}−(O_2^{2-})−Cu^{II} complexes (**1**−**4**) under study were generated by bubbling excess dioxygen through − 80 or − 40 °C (depending on the solvent) solutions of either the 1:1 mixture of reduced (F_8)Fe^{II} and Cu^{I}(ligand) complexes (**1** and **3**) or the heterobinuclear complexes [(^{6}L)Fe^{II}···Cu^{I}]$^+$ (**2**) or [(^{2}L)Fe^{II}···Cu^{I}]$^+$ (**4**) (Chart 1). Previous studies, along with current observations on the new complex **3**, show that these Fe^{III}−(O_2^{2-})−Cu^{II} complexes fully form and that this process is irreversible in that application of a vacuum or bubbling with Ar to the low-temperature complex solutions will not cause O_2 release.[17,21,23] The reactivity studies were carried out at low-temperatures because the peroxo complexes are thermally unstable, transforming cleanly to the corresponding μ-oxo species (i.e., Fe^{III}−O−Cu^{II},[40−42] for all but complex **4**). Prior to the addition of reagents for reactivity investigations, excess O_2 was removed through the application of vacuum/Ar purges.

Reactions with CO. Carbon monoxide has been extensively used in biological studies on metalloproteins and, in particular, on heme/Cu oxidases, as a probe or surrogate for active-site dioxygen binding.[5] For example, CO binds to the heme in reduced cytochrome *c* oxidase, and many biochemical/biophysical investigations employ the heme−CO adduct to initiate laser photoejection of carbon monoxide to probe binding to Cu_B (with subsequent deligation and rebinding to Fe^{II}), perturbation/motions/proton movements in the heme−Cu surrounding, or both.[43−46] Carbon monoxide is known to give CO_2 in a reaction with reductively activated (with O_2) C*c*O, and the nature of the enzyme intermediates involved have recently been probed using resonance Raman spectroscopy.[47] Furthermore, CO is well-known to strongly bind to five-coordinated ferrous heme proteins, as well as in small molecule synthetic analogues.[31,48] Rather than an examination of reduced complex/CO interactions (for which we separately have information),[49] the reaction of **1**−**4** with CO may reveal if peroxide can be displaced (as O_2), that is, if CO is thermodynamically a better ligand (than O_2) for the reduced heme or copper center. In addition, insights into how copper and iron work synergistically in these heme−copper environments may be revealed. Indeed, we find that **1** does not react with CO, while for **2**−**4**, the peroxo group is displaced via redox reactions.

(39) Liang, H.-C.; Zhang, C. X.; Henson, M. J.; Sommer, R. D.; Hatwell, K. R.; Kaderli, S.; Zuberbuehler, A. D.; Rheingold, A. L.; Solomon, E. I.; Karlin, K. D. *J. Am. Chem. Soc.* **2002**, *124*, 4170−4171.
(40) Karlin, K. D.; Nanthakumar, A.; Fox, S.; Murthy, N. N.; Ravi, N.; Huynh, B. H.; Orosz, R. D.; Day, E. P. *J. Am. Chem. Soc.* **1994**, *116*, 4753−4763.
(41) Ju, T. D.; Ghiladi, R. A.; Lee, D.-H.; van Strijdonck, G. P. F.; Woods, A. S.; Cotter, R. J.; Young, J. V. G.; Karlin, K. D. *Inorg. Chem.* **1999**, *38*, 2244−2245.
(42) The X-ray structure of [(F_8)Fe^{III}-O-Cu^{II}(AN)]$^+$ will be described elsewhere.
(43) Yoshikawa, S.; Shinzawa-Itoh, K.; Nakashima, R.; Yaono, R.; Yamashita, E.; Inoue, N.; Yao, M.; Jei-Fei, M.; Libeu, C. P.; Mizushima, T.; Yamaguchi, H.; Tomizaki, T.; Tsukihara, T. *Science* **1998**, *280*, 1723−1729.
(44) Koutsoupakis, C.; Pinakoulaki, E.; Stavrakis, S.; Daskalakis, V.; Varotsis, C. *Biochim. Biophys. Acta* **2004**, *1655*, 347.
(45) Einarsdottir, O.; Szundi, I. *Biochim. Biophys. Acta* **2004**, *1655*, 263.
(46) McMahon, B. H.; Fabian, M.; Tomson, F.; Causgrove, T. P.; Bailey, J. A.; Rein, F. N.; Dyer, R. B.; Palmer, G.; Gennis, R. B.; Woodruff, W. H. *Biochim. Biophys. Acta* **2004**, *1655*, 321.
(47) Kim, Y.; Shinzawa-Itoh, K.; Yoshikawa, S.; Kitagawa, T. *J. Am. Chem. Soc.* **2001**, *123*, 757−758.
(48) Silvernail, N. J.; Roth, A.; Schulz, C. E.; Noll, B. C.; Scheidt, W. R. *J. Am. Chem. Soc.* **2005**, *127*, 14422−14433.
(49) Kretzer, R. M.; Ghiladi, R. A.; Lebeau, E. L.; Liang, H.-C.; Karlin, K. D. *Inorg. Chem.* **2003**, *42*, 3016−3025.

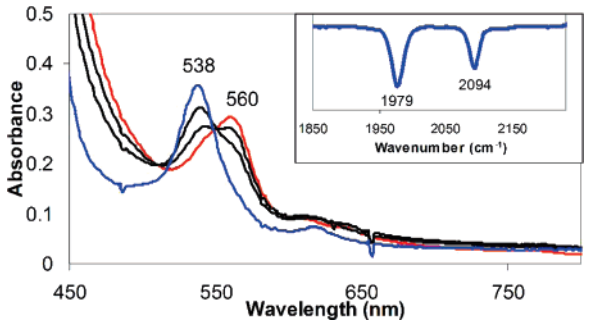

Figure 3. UV−vis spectra monitoring the reaction of $[(^6L)Fe^{III}\text{-}(O_2^{2-})\text{-}Cu^{II}]^+$ (**2**) (red, $\lambda_{max} = 560$ nm) with CO in CH_3CN at −40 °C, producing $[(^6L)Fe^{II}-CO\cdots Cu^{I}-CO]^+$ (blue, $\lambda_{max} = 538$ nm). Spectra shown in black are generated during the transformation, the first obtained immediately and the second after 5 min of bubbling CO. Inset: IR spectrum of $[(^6L)Fe^{II}-CO\cdots Cu^{I}-CO]^+$ in CH_3CN; the complete IR spectrum is given in Supporting Information.

Scheme 2

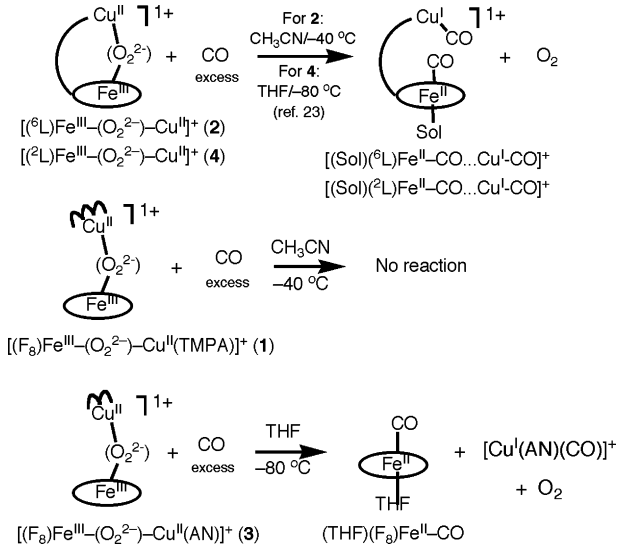

$[(^6L)Fe^{III}-(O_2^{2-})-Cu^{II}]^+$ (**2**) was found to react with CO to form the bis(carbon monoxide) adduct $[(solvent)(^6L)Fe^{II}-CO\cdots Cu^{I}\text{-}CO]^+$ (Scheme 2); as shown earlier, the heme−CO moiety is also solvent bound leading to an overall six-coordinate low-spin complex.[49] When CO was bubbled through an acetonitrile solution of **2** at − 40 °C, the Q-band absorption at 560 nm, corresponding to **2**, blue-shifted to 538 nm (Figure 3), which is the Q-band position independently determined for $[(CH_3CN)(^6L)Fe^{II}-CO\cdots Cu^{I}-CO]^+$ via CO exposure to the reduced complex $[(^6L)Fe^{II}\cdots Cu^{I}]^+$.[49] Solution IR spectra (in CH_3CN) confirmed that CO is bound to both metals (Figure S2),[50] as evidenced by the presence of two ν(C−O) stretching bands, at 2094 cm^{-1} ($Cu^{I}-CO$) and 1979 cm^{-1} ($Fe^{II}-CO$), values typical for copper−carbonyl[5,51] and reduced heme−CO[5,31,49] coordination complexes and metalloproteins. The same behavior was previously observed and described for $[(^2L)Fe^{III}-(O_2^{2-})-Cu^{II}]^+$ (**4**), and evolution of O_2 was detected (Scheme 2).[23]

Surprisingly, there is no reaction between $[(F_8)Fe^{III}-(O_2^{2-})-Cu^{II}(TMPA)]^+$ (**1**) and CO (after vigorous bubbling for 2−5 min). By comparison to the positive reaction with CO observed for $[(^6L)Fe^{III}-(O_2^{2-})-Cu^{II}]^+$ (**2**) (vide supra), which possesses the similar tetradentate TMPA Cu chelate, this result suggests that the bonding at the metal−peroxo core in **2** is weaker than that in **1**. This may be because of the nature of the binucleating ^6L ligand in **2**, with linker to one pyridyl group of the TMPA moiety, which leads to ligand constraints translating to distortions from optimal coordination geometry.[41] In fact, in detailed CO binding studies to reduced complex $[(^6L)Fe^{II}\cdots Cu^{I}]^+$, we previously published that the ligand constraints lead to the major species $[(solvent)\text{-}(^6L)Fe^{II}-CO\cdots Cu^{I}-CO]^+$ possessing *tridentate* chelation within the $Cu^{I}-CO$ moiety (see diagram below), as deduced from ν_{C-O} IR data in comparison to known complexes.[49] In other words, **2** behaves more like it has tridentate chelation to copper.

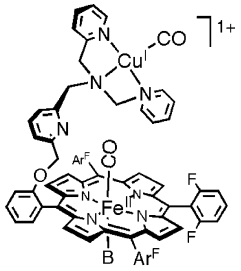

$[(^6L)Fe^{II}\text{-}CO\ldots Cu^{I}\text{-}CO]^+$

Along with the CO reactions seen with **2** and **4**, $[(F_8)\text{-}Fe^{III}\text{-}(O_2^{2-})\text{-}Cu^{II}(AN)]^+$ (**3**)/CO gives corresponding chemistry (Scheme 2 and Figure S3 (UV−vis monitoring)). Bubbling CO through solutions of **3** at −80 °C leads to the formation of a UV−vis spectrum[50] typical of a heme−carbonyl complex.[49,52] We also characterized the reaction products (Scheme 2) by IR spectroscopy; the expected heme−carbonyl is formed (ν(C−O) = 1982 cm^{-1}),[49,52] along with $[(AN)Cu^{I}-CO]^+$ (ν(C−O) = 2077 cm^{-1}), and the latter result was confirmed by comparison with the CO adduct formed starting with authentic $[(AN)Cu^{I}]^+$.[50] This finding is interesting in regards to the tridentate (AN)Cu chelate present in **3**, again by comparison to having a tetradentate TMPA chelate in **1**. The results suggest that the metal−peroxo core bonding in **1** (known to have $\mu\text{-}\eta^2\text{:}\eta^1$ peroxo ligation, Chart 1) is stronger than would be found in **3** with side-on side-on $\mu\text{-}\eta^2\text{:}\eta^2$ peroxo bonding. This seems surprising to us, and we propose that the favorable CO reactivity with **3** reflects stronger CO bonding in the resulting complex $[(AN)Cu^{I}-CO]^+$ compared to that in $[(TMPA)Cu^{I}-CO]^+$. In support of this supposition, it is qualitatively very difficult to remove (by vacuum purge, Ar bubbling, or both) the CO in $[(AN)\text{-}Cu^{I}-CO]^+$ or other tridentate ligand $Cu^{I}-$complexes,[53,54] while $[(TMPA)Cu^{I}-CO]^+$ readily loses carbon monoxide.[49] Further investigations which can provide thermodynamic data on heme−peroxo−copper and ligand−$Cu^{I}-CO$ complex stabilities would be needed to obtain further insights.

(50) See Supporting Information.

(51) Rondelez, Y.; Séneque, O.; Rager, M.-N.; Duprat, A. F.; Reinaud, O. *Chem.—Eur. J.* **2000**, *6*, 4218−4226.
(52) Thompson, D. W.; Kretzer, R. M.; Lebeau, E. L.; Scaltrito, D. V.; Ghiladi, R. A.; Lam, K.-C.; Rheingold, A. L.; Karlin, K. D.; Meyer, G. J. *Inorg. Chem.* **2003**, *42*, 5211−5218.

Reactions with PPh_3. Phosphines such as PPh_3 are also interesting probes of metal−peroxo complexes because, as is similar to carbon monoxide, they bind well to low-valent (reduced) metal ions such as Fe(II)[55] and copper(I).[56−61] In contrast to CO, PPh_3 may in some cases be readily oxygenated to give O=PPh_3. However, it is already known that mononuclear side-on bound peroxo−iron(III)−porphyrin complexes do not oxidize PPh_3;[29] thus, we wondered if now when the peroxide ligand also coordinates copper(II) ion, it may be capable of phosphine oxidation. Indeed, with differently coordinated peroxo−dicopper(II) complexes, PPh_3 can either lead to displacement of the peroxo ligand (as O_2), accompanied by ligand−Cu^I−PPh_3 formation, or alternatively undergo oxidation.[28,57−61]

Interestingly, $[(F_8)Fe^{III}\text{-}(O_2^{2-})\text{-}Cu^{II}(AN)]^+$ (**3**) reacts with PPh_3 to displace the peroxo ligand from copper, but not from iron, thus with formally a partial reduction reaction. The products are the iron−superoxo species (solvent)(F_8TPP)-$Fe^{III}-(O_2^-)$ (UV−vis identification, λ_{max} = 417 and 531 nm)[37,38] and the reduced Cu^I−phosphine adduct $[Cu^I(AN)(PPh_3)]^+$ (Scheme 3 and Figure 4). Tridentate N_3- and tetradentate N_4-ligand−Cu^I complexes readily form PPh_3 adducts.[57,58,61] Direct evidence for the presence of $[Cu^I(AN)(PPh_3)]^+$ was not straightforward; however ^{31}P NMR spectroscopic interrogation of the product solutions showed only the presence of PPh_3 (and no O=PPh_3).[62] The same behavior was previously observed and documented for PPh_3 reaction with $[(^2L)Fe^{III}\text{-}(O_2^{2-})\text{-}Cu^{II}]^+$ (**4**),[23] see Scheme 3.

Unexpectedly, with complexes possessing the TMPA tetradentate ligand on copper, $[(F_8)Fe^{III}\text{-}(O_2^{2-})\text{-}Cu^{II}(TMPA)]^+$ (**1**) and $[(^6L)Fe^{III}\text{-}(O_2^{2-})\text{-}Cu^{II}]^+$ (**2**), there is no reaction toward PPh_3. There are no UV−vis changes, and ^{31}P NMR spectroscopy confirms that *no* PPh_3 oxidation has occurred (see Experimental Section). $[Cu^I(TMPA)(PPh_3)]^+$ is a known compound with a described X-ray structure, and PPh_3 displaces O_2 from the well-known μ-1,2-peroxo dicopper-(II) complex $[(TMPA)Cu^{II}\text{-}(O_2^{2-})\text{-}Cu^{II}(TMPA)]^{2+}$.[27,28,61] However, the observations here suggest the overall peroxo−metal core (i.e., $Fe^{III}-(O_2^{2-})-Cu^{II}$) bonding in **1** and **2** is stronger

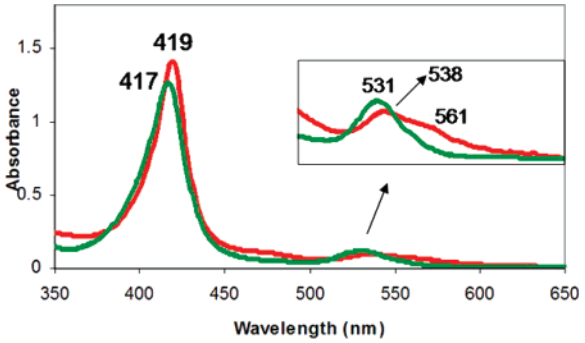

Figure 4. UV−vis spectra for the reaction of $[(F_8)Fe^{III}\text{-}(O_2^{2-})\text{-}Cu^{II}(AN)]^+$ (**3**) (red, λ_{max} = 419 (Soret), 538, 561 nm) with 5 equiv of PPh_3 in THF at −80 °C. The product is $(F_8)Fe^{III}-(O_2^-)$ (green, λ_{max} = 417 (Soret), 531 nm), identified by comparison with an authentic sample.[37,38]

Scheme 3

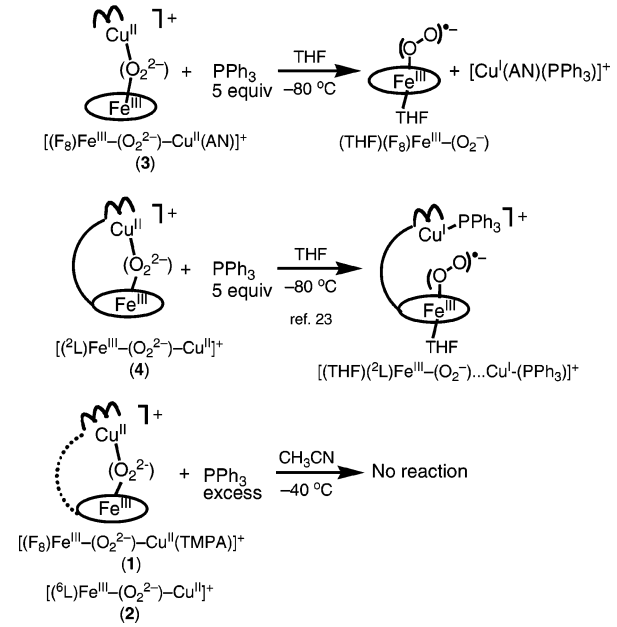

than that in $[(TMPA)Cu^{II}-(O_2^{2-})-Cu^{II}(TMPA)]^{2+}$, despite the similar end-on binding to copper(II). Surprisingly (to us), **3** and **4** with their side-on η^2-peroxo-Cu ligation (i.e., two-bonds to Cu(II)) readily undergo reactions with PPh_3 (Scheme 3). More insights are needed.[63]

Overall, with respect to CO and PPh_3 binding, which compete for the peroxo iron or copper ligation, complex $[(F_8)Fe^{III}\text{-}(O_2^{2-})\text{-}Cu^{II}(TMPA)]^+$ (**1**) appears to be the most stable heme−peroxo−copper complex of the four being studied.

Reactions with Acids. Protonation studies of peroxo-bridged iron−copper synthetic models of heme−copper oxidases are of particular importance because the O−O cleavage process is assisted by 1 or 2 equiv of protons in

(53) Karlin, K. D.; Haka, M. S.; Cruse, R. W.; Meyer, G. J.; Farooq, A.; Gultneh, Y.; Hayes, J. C.; Zubieta, J. *J. Am. Chem. Soc.* **1988**, *110*, 1196−1207.
(54) Zhang, C. X.; Liang, H.-C.; Kim, E.-i.; Shearer, J.; Helton, M. E.; Kim, E.; Kaderli, S.; Incarvito, C. D.; Zuberbühler, A. D.; Rheingold, A. L.; Karlin, K. D. *J. Am. Chem. Soc.* **2003**, *125*, 634−635.
(55) Simonneaux, G. *Coord. Chem. Rev.* **1997**, *165*, 447−474.
(56) Jardine, F. H. *Adv. Inorg. Chem. Radiochem.* **1975**, *17*, 115−163.
(57) Karlin, K. D.; Cruse, R. W.; Gultneh, Y.; Farooq, A.; Hayes, J. C.; Zubieta, J. *J. Am. Chem. Soc.* **1987**, *109*, 2668−2679.
(58) Karlin, K. D.; Ghosh, P.; Cruse, R. W.; Farooq, A.; Gultneh, Y.; Jacobson, R. R.; Blackburn, N. J.; Strange, R. W.; Zubieta, J. *J. Am. Chem. Soc.* **1988**, *110*, 6769−6780.
(59) Karlin, K. D.; Gan, Q.-F.; Farooq, A.; Liu, S.; Zubieta, J. *Inorg. Chim. Acta* **1989**, *165*, 37−39.
(60) Karlin, K. D.; Tyeklár, Z.; Farooq, A.; Haka, M. S.; Ghosh, P.; Cruse, R. W.; Gultneh, Y.; Hayes, J. C.; Toscano, P. J.; Zubieta, J. *Inorg. Chem.* **1992**, *31*, 1436−1451.
(61) Tyeklár, Z.; Jacobson, R. R.; Wei, N.; Murthy, N. N.; Zubieta, J.; Karlin, K. D. *J. Am. Chem. Soc.* **1993**, *115*, 2677−2689.
(62) The triphenylphosphine added to complex **3** either remains free in solution or coordinated as $[Cu^I(AN)(PPh_3)]^+$, which leads to some observed line broadening of the ^{31}P-NMR resonance of PPh_3, as we have previously described in detail for the chemistry of complex **4**, see ref 23.
(63) A reviewer suggested perhaps the lack of reactivity of **1** and **2** with PPh_3 could be caused by sterics. We see this as being unlikely because, as already noted in the text, PPh_3 reacts readily with the very bulky complexes **3** and **4** and with the peroxodicopper(II) complex with TMPA ligand. We tried a reaction of **1** with PMe_3 (1 and then 2 equiv), and even with one equivalent, an immediate reaction leading to the bisphosphine heme−iron(II) compound (UV-vis monitoring) occurs, as confirmed by separate control experiments. Thus, a totally different chemistry occurs with PMe_3, undoubtedly because its very strong Lewis basicity and reducing capacity.

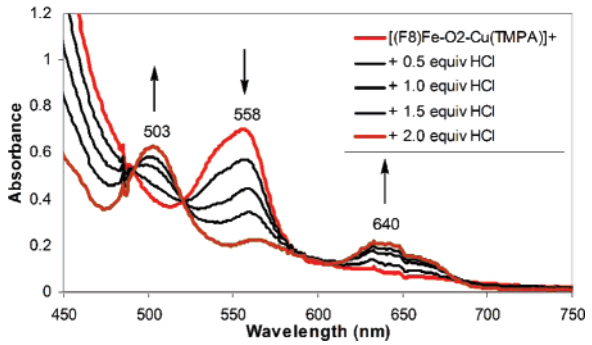

Figure 5. UV−vis spectra for the reaction of $[(F_8)Fe^{III}\text{-}(O_2^{2-})\text{-}Cu^{II}\text{-}(TMPA)]^+$ (**1**) (red, λ_{max} = 558 nm) with 2 equiv of HCl in CH_3CN at −40 °C. The brown spectrum of the final product is dominated by the absorption features distinctive to $(F_8)Fe^{III}$−Cl (λ_{max} = 503, 567, 640 nm), also identified by comparison with an authentic sample.[40]

the key enzymatic O−O cleavage step, **A** → ferryl (Fe^{IV}═O···Cu^{II}−OH^- species) (see Introduction and some further comments below).[14−16] A hydroperoxo transient intermediate (following electron-transfer reduction of **A** and subsequent protonation) has also been at times invoked, and generation of such a species by protonation of complexes **1**−**4** would be of great fundamental interest.[15,64] Furthermore, protonation studies on synthetic models may afford insights relating to the intricate C*c*O proton membrane translocation mechanism, which is coupled to the O_2-reductive cleavage.[32,65]

The basic nature of the peroxo ligand in all four Fe^{III}−peroxo−Cu^{II} compounds under study (**1**−**4**) is revealed in the reaction with Brønsted acids. For example, the addition of two or more equivalents of HCl to a solution of **1** at −40 °C cleanly gives $(F_8)Fe^{III}$-Cl, as revealed by formation of its distinctive UV−vis spectrum (see "titration" in MeCN solvent, with isosbestic behavior, Figure 5). There is no evidence for any hydroperoxo compound intermediate (but see discussion below).

Low-temperature ^{1}H NMR spectroscopy was also employed to provide more insights and hopefully unveil information concerning other reaction products. Figure 6 reveals the clean transformation of the $[(F_8)Fe^{III}\text{-}(O_2^{2-})\text{-}Cu^{II}\text{-}(TMPA)]^+$ (**1**) to two mononuclear products, again $(F_8)Fe^{III}$-Cl, along with $[Cu^{II}(TMPA)Cl]^+$, upon titration of **1** with HCl in CD_3CN at −40 °C (also, see Experimental Section). With 1 equiv of HCl, the signals corresponding to the two *meta* and one *para* phenyl hydrogens of the peroxo complex **1** (red asterisk) diminish in intensity, while new resonances arise, attributed to the *meta* and *para* phenyl protons of (F_8)-Fe^{III}-Cl (green asterisks). In addition, the 4-pyridyl hydrogen resonance assignable to $[Cu^{II}(TMPA)Cl]^+$ now appears (blue asterisk).[66] These assignments were confirmed by obtaining spectra of authentic materials under the same conditions of solvent and temperature.[67] After the addition of 2 equiv of

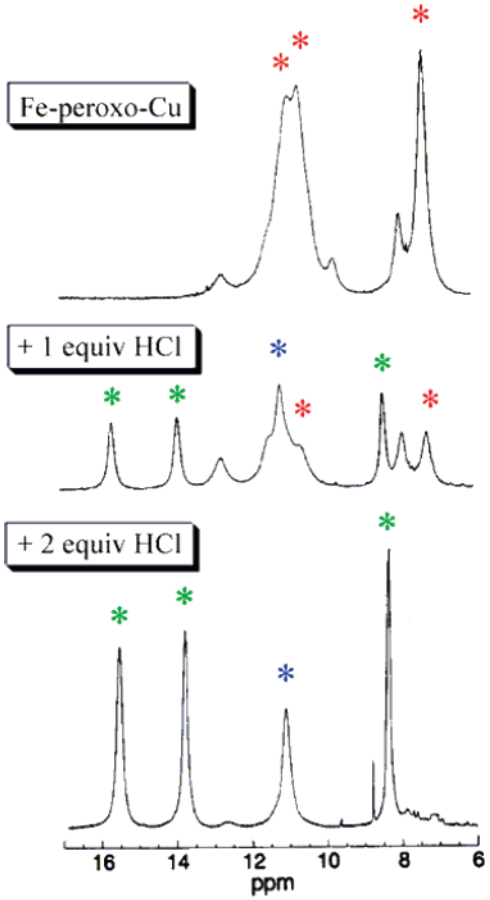

Figure 6. Reaction of $[(F_8)Fe^{III}\text{-}(O_2^{2-})\text{-}Cu^{II}(TMPA)]^+$ (**1**) with HCl in CD_3CN at −40 °C, followed by ^{1}H NMR spectroscopy (only the 6−17 nm "diamagnetic" region is shown): red asterisk, phenyl hydrogens of **1**; green asterisk, phenyl hydrogens of $(F_8)Fe^{III}$−Cl; blue asterisk, 4-pyridyl hydrogens of $[Cu^{II}(TMPA)Cl]^+$. See text for further explanation.

HCl, the changes in the spectra indicate the reaction is complete (Figure 6).[68] The results show that no hydroperoxo species is detected under these conditions.

Hydrogen peroxide as a coproduct was not detected by NMR spectroscopy (a peak may be expected at ∼9.5 ppm).[69] However, H_2O_2 was quantitatively determined spectrophotometrically as a peroxotitanyl species.[70,71] After the addition of 10 equiv of HCl (an excess, to optimize this analytical procedure), H_2O_2 was found to be produced in a 70% yield from $[(F_8)Fe^{III}\text{-}(O_2^{2-})\text{-}Cu^{II}(TMPA)]^+$ (**1**) (See Experimental Section).

To support the results found by ^{1}H NMR spectroscopy, the reaction of $[(F_8)Fe^{III}\text{-}(O_2^{2-})\text{-}Cu^{II}(TMPA)]^+$ (**1**) with HCl was also investigated by EPR spectroscopy and ESI-MS. When studied in CH_3CN at −40 °C, aliquots from the reaction solution were frozen, and EPR spectra were

(64) Collman, J. P.; Decréau, R. A.; Sunderland, C. J. *Chem. Commun.* **2006**, 3894−3896.
(65) Fox, S.; Nanthakumar, A.; Wikström, M.; Karlin, K. D.; Blackburn, N. J. *J. Am. Chem. Soc.* **1996**, *118*, 24−34.
(66) Nanthakumar, A.; Fox, S.; Murthy, N. N.; Karlin, K. D. *J. Am. Chem. Soc.* **1997**, *119*, 3898−3906.
(67) $[Cu^{II}(TMPA)(CH_3CN)]^{2+}$ was used as the reference compound for the ^{1}H NMR assignment.
(68) A downfield broad absorption assigned to the pyrrole hydrogens of **1** (see ref 17) decreases in intensity as the new peak at 100 ppm (due to the high-spin $(F_8)Fe^{III}$-Cl complex) grows (data not shown). In addition, 3- and 5-pyridyl hydrogens at ∼35 ppm (broad), due to Cu^{II}(TMPA) (see ref 66), grow (data not shown).
(69) Shearer, J.; Scarrow, R. C.; Kovacs, J. A. *J. Am. Chem. Soc.* **2002**, *124*, 11709−11717.
(70) Eisenberg, G. M. *Ind. Eng. Chem.—Anal. Ed.* **1943**, *15*, 327−328.
(71) Chaudhuri, P.; Hess, M.; Mueller, J.; Hildenbrand, K.; Bill, E.; Weyhermueller, T.; Wieghardt, K. *J. Am. Chem. Soc.* **1999**, *121*, 9599−9610.

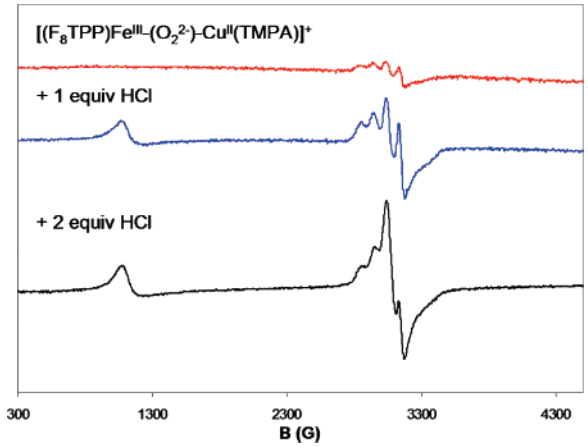

Figure 7. Reaction of [(F$_8$)Fe^{III}-(O$_2^{2-}$)-Cu^{II}(TMPA)]$^+$ (**1**) with HCl in CH$_3$CN at −40 °C, followed by EPR spectroscopy. Spectrum of **1** (red, "silent" but with a small Cu^{II}(TMPA) impurity, upper spectrum) and after the addition of 1 equiv of HCl (blue, middle spectrum) showing the spectra associated with the Fe^{III}−Cl and Cu^{II}−Cl complexes. The lower spectrum (black) is associated with addition of 2 equiv of HCl, and small distortions in the upfield copper(II) signal occur when excess HCl is present, see Supporting Information: frequency, 9.192 GHz; temperature, 77 K; time constant, 10.24 ms; sweep width, 4200 G. See text for further explanations.

recorded. As shown in Figure 7, the original **1** is EPR silent because of the strong antiferromagnetic coupling between the high-spin iron(III) and copper(II) ions.[19] After the addition of 1 equiv of HCl, a spectrum with two major components is obtained: one occurs at $g = 5.8$, and the other, a copper(II) signal, occurs near $g = 2$. The signal in the low-field region of the spectrum is attributed to the perpendicular contribution of the high-spin (F$_8$)Fe^{III}−Cl (with the expected low-intensity parallel signal at $g \approx 2.00$ being overlapped by the strong signal of the copper(II) complex). In fact, the higher-field copper(II) signal is distinctive ($g_{||} = 2.08$, $g_{\perp} = 2.18$, $A_{\perp} = 91 \times 10^{-4}$ cm^{-1}; a "reverse" axial EPR signal ($g_{||} < g_{\perp}$) that is expected for trigonal-bypyramidal complexes with the TMPA ligand, namely, [Cu^{II}(TMPA)(X)]$^{y+}$ (X = CH$_3$CN or Cl$^-$, Figure 7)).[72] The addition of the second equivalent of HCl completes the reaction as shown by the development of more intense signals for the chloride complexes of both iron and copper. ESI-MS investigation supports the EPR conclusions concerning the copper complex product; a prominent signal at m/z = 388.38 and simulation of the signal envelope around this corresponds to [Cu^{II}(TMPA)Cl]$^+$ (Figure S7).[50]

We also carried out the protonation of [(F$_8$)Fe^{III}-(O$_2^{2-}$)-Cu^{II}(TMPA)]$^+$ (**1**) in CH$_2$Cl$_2$ to corroborate the above findings; we were concerned if CH$_3$CN as solvent and known ligand for iron and copper (in oxidized or reduced states) might influence the chemistry. This was not the case because dissolution of solid peroxo complex **1** (see Experimental Section) in CH$_2$Cl$_2$ and monitoring of the HCl reactivity by UV−vis spectroscopy gave the same results (see Supporting Information, Figure S8).

From the observations thus far described, it is clear that the protonation reactions are strongly influenced by the presence of the chloride counterion, with its high affinity for iron(III) and copper(II) ions; consequently, (F$_8$)Fe^{III}−Cl and [Cu^{II}(TMPA)Cl]$^+$ are formed (vide supra). However, the

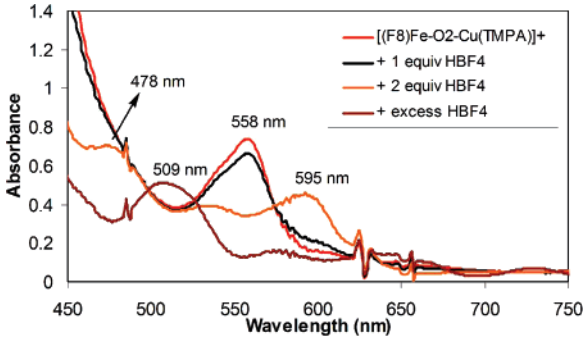

Figure 8. UV−vis spectra for the reaction of [(F$_8$)Fe^{III}-(O$_2^{2-}$)-Cu^{II}-(TMPA)]$^+$ (**1**) (red, λ_{max} = 558 nm) with tetrafluoroboric acid (HBF$_4$) in CH$_3$CN at −40 °C. The orange spectrum is assigned to (F$_8$)Fe^{III}−F (λ_{max} = 478, 535, 595 nm), while the brown spectrum (final product) corresponds to (F$_8$)Fe^{III}−(BF$_4$) (λ_{max} = 509, ∼580, ∼640 nm).[73] See text for further discussion.

addition of 2 equiv of *tert*-butylammonium chloride (as a source of chloride) to **1** does not yield the expected (F$_8$)-Fe^{III}−Cl (only ∼ 20% conversion to the μ-oxo analogue [(F$_8$)Fe^{III}-O-Cu^{II}(TMPA)]$^+$ is observed, UV−vis monitoring), revealing that the reaction driving force is not only chloride but also the proton.

To gain more insights on the effect of the counterion, we also carried out protonation experiments with [(F$_8$)Fe^{III}-(O$_2^{2-}$)-Cu^{II}(TMPA)]$^+$ (**1**) using triflic (HOTf) and tetrafluoroboric acids. The reaction of **1** with HOTf acid in CH$_3$CN at −40 °C yields the compound identified as (F$_8$)Fe^{III}−OTf (Figure S9)[50] because triflate is also a good ligand for iron-(III).[73] Surprisingly, we did not observe the expected Cu products, [Cu^{II}(TMPA)(X)]$^{y+}$ (X = OTf$^-$ or CH$_3$CN), but ESI-MS interrogation revealed that the only product is [Cu^{II}-(TMPA)(CN)]$^+$ (m/z = 379.36, confirmed by simulation, Figure S10);[50] this complex has been previously synthesized and characterized by X-ray diffraction.[74] Further investigation of the nature of this reaction will be carried out and reported elsewhere. We surmise that the solvent acetonitrile is the cyanide source following its oxidation, possibly by a copper−hydroperoxo species which forms upon protonation of **1**; we have separately documented such a reaction effected by a hydroperoxo−dicopper(II) complex.[75]

The result of the reaction of **1** with HBF$_4$ was quite different. After the addition of two equiv of HBF$_4$, we observed a new UV−vis spectrum (Figure 8), assigned to (F$_8$)Fe^{III}−F [λ_{max} (CH$_3$CN) = 478, 530, 595 nm], because of its similarity to the UV−vis spectrum of the analogue (OEP)Fe^{III}−F [λ_{max} (CH$_2$Cl$_2$) = 485, 510, 600 nm].[76] We considered the possibility that a fluoride-bridged complex formed, that is, [(F$_8$)Fe^{III}-F−Cu^{II}(TMPA)]$^{2+}$, which would be an analogue to the known compound [(OEP)Fe^{III}−F−Cu^{II}(bnpy$_2$)(CH$_3$CN)]$^+$ {OEP = octaethylporphyrinate; bnpy

(72) Lucchese, B.; Humphreys, K. J.; Lee, D.-H.; Incarvito, C. D.; Sommer, R. D.; Rheingold, A. L.; Karlin, K. D. *Inorg. Chem.* **2004**, *43*, 5987−5998.
(73) Boersma, A. D.; Goff, H. M. *Inorg. Chem.* **1982**, *21*, 581−586.
(74) Corsi, D. M.; Murthy, N. N.; Young, J. V. G.; Karlin, K. D. *Inorg. Chem.* **1999**, *38*, 848−858.
(75) Li, L.; Sarjeant, A. A. N.; Karlin, K. D. *Inorg. Chem.* **2006**, *45*, 7160−7172.
(76) Lee, S. C.; Holm, R. H. *Inorg. Chem.* **1993**, *32*, 4745−4753.

= *N*,*N*-bis(2-(2-pyridylethyl))benzylamine}.[76] However, this can be ruled out because EPR spectroscopy (Figure S11)[50] reveals distinctive signals for both uncoupled heme (i.e., mononuclear Fe^{III} high-spin) and copper complexes; EPR spectra of a heme−F−Cu^{II} coupled system show distinctively different resonances.[77,78] As would be expected, the addition of excess HBF_4 yields the mononuclear $(F_8)Fe^{III}$−(BF_4) complex (Figure 8).[73] The overall results with HBF_4 addition to heme−peroxo−copper complex **1** show that BF_4^- as counterion acts as a reactive source of fluoride (as is well-known),[76] and this is responsible for part of observed chemistry. As concerns the copper complex product in the HBF_4 + **1** reaction, an analogous result to that seen with triflic acid was observed. The only product detected, by ESI-MS, was the same cyanide complex $[Cu^{II}(TMPA)(CN)]^+$ (m/z = 379.46),[50] and we suggest similar chemistry (vide supra) is occurring here.

To summarize, the counterions chloride, triflate, and tetrafluoroborate (by itself or providing fluoride) are playing key roles in the reactions of heme−peroxo−copper complex of $[(F_8)Fe^{III}\text{-}(O_2^{2-})\text{-}Cu^{II}(TMPA)]^+$ (**1**) with HCl, HOTf, and HBF_4, respectively. The HCl reactions are quite clean, giving chloride−metal products, but for the other acids with weak ligand counterions, additional chemistry occurs. As mentioned, HBF_4 causes the $(F_8)Fe^{III}$−F complex to form. With either HBF_4 or HOTf, some new chemistry occurs leading to cyanide production and ready formation of $[Cu^{II}(TMPA)\text{-}(CN)]^+$. In the probe for production of hydrogen peroxide by HCl reaction with **1**, this occurs in a near stoichiometric fashion. However, with HOTf and HBF_4, we could not confirm any H_2O_2 formation with the titanyl oxo-sulfate reagent because of spectroscopic interference with aqueous acetonitrile soluble heme complexes or other chemical reactions leading to new strongly absorbing species. In fact, we would not expect hydrogen peroxide to be left over because it would be used up in the CH_3CN oxidation and cyanide formation.[75]

As is relevant to the discussion above concerning protonation of $[(F_8)Fe^{III}\text{-}(O_2^{2-})\text{-}Cu^{II}(TMPA)]^+$ (**1**), we mention here preliminary observations with $[H(Et_2O)_2][B(C_6F_5)_4]$[79] as our acid source, with its non-coordinating perfluorinated tetraarylborate counteranion. Reaction of **1** with 1 equiv of $[H(Et_2O)_2][B(C_6F_5)_4]$ at − 40 °C in CH_3CN indeed leads to a new UV−vis spectrum (see Supporting Information, Figure S13). In parallel, reaction of **1** with one equiv of trimethyloxonium tetrafluoroborate (as a proton analogue methylating reagent) gave essentially the same UV−vis spectrum. We speculate that the new species (based on UV−vis criterion) are hydro- or methyl-peroxo complexes Fe^{III}−(μ-^-O_2R)−Cu^{II} or Fe^{III}−(^-O_2R)···Cu^{II}, R = H or Me. Future investigations will focus on further characterization of these interesting and potentially important species.

Scheme 4

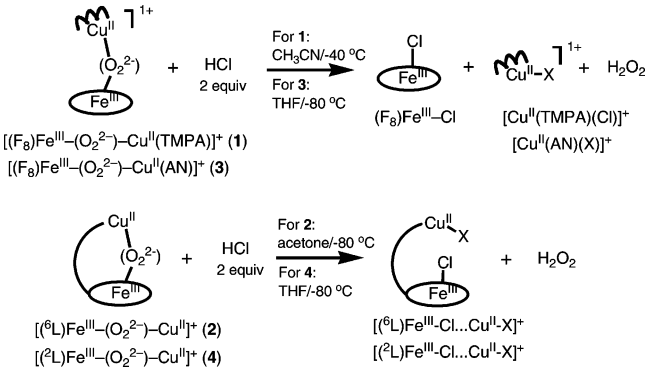

Scheme 5

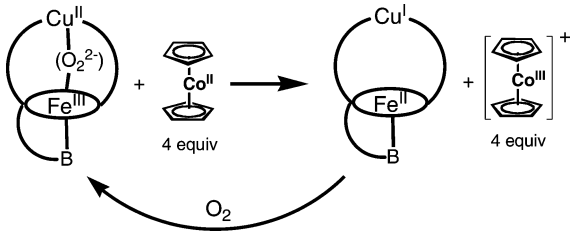

We now very briefly summarize the similar results observed for the other complexes **2**−**4** (Scheme 4). They all react with HCl to give a (porphyrinate)Fe^{III}−Cl moiety (as judged by UV−vis or ^{1}H NMR spectroscopies, see Experimental Section and Supporting Information, Figures S14−S16) liberating hydrogen peroxide, in 80% yield from **2** and 77% yield from **3**. The yield in the reaction of **4** with HCl was not determined.

Reactions with Cobaltocene. The full reductive cleavage of dioxygen to water requires four electron equivalents. However, in our present C*c*O model complexes **1**−**4**, dioxygen has been reduced only by two-electrons to the peroxo level and is coordinated by a high-spin iron(III) and copper(II) ion. In this section, we report the reactivity of peroxo compounds **1**−**4** toward cobaltocene ($CoCp_2$), a strong one-electron outer-sphere reductant.[80] Can the addition of one or two *more* reducing equivalents lead to O−O reductive cleavage and what will occur? Part of the reason for examining this reaction is the prior work of Collman and co-workers[33−36] where they showed that heme−peroxo−copper complexes with added $Co(Cp)_2$ lead to fully reduced Fe^{II}/Cu^{I} compounds (Scheme 5). We wished to compare and contrast such behavior with our own series of complexes.

In fact, the reaction of **1** and **2** with cobaltocene has been previously described in earlier reports.[21,81] As shown in Scheme 6, the addition of two or more equiv of $CoCp_2$ to a solution of **1** or **2** yields the corresponding structurally characterized μ-oxo-bridged compounds $[(F_8)Fe^{III}\text{-O-}Cu^{II}\text{-}(TMPA)]^+$[40] and $[(^6L)Fe^{III}\text{-O-}Cu^{II}]^+$,[41] respectively. Here, we add to this information and report on the other cases. For the reaction with **1**, cobaltocinium cation ($[Co^{III}Cp_2]^+$, Scheme 6) was directly observable by UV−vis spectroscopy,

(77) Oganesyan, V. S.; Butler, C. S.; Watmough, N. J.; Greenwood, C.; Thomson, A. J.; Cheesman, M. R. *J. Am. Chem. Soc.* **1998**, *120*, 4232−4233.
(78) Watmough, N. J.; Cheesman, M. R.; Gennis, R. B.; Greenwood, C.; Thomson, A. J. *FEBS Lett.* **1993**, *319*, 151−154.
(79) Jutzi, P.; Muller, C.; Stammler, A.; Stammler, H. G. *Organometallics* **2000**, *19*, 1442−1444.
(80) Connelly, N. G.; Geiger, W. E. *Chem. Rev.* **1996**, *96*, 877−910.
(81) Chufán, E. E.; Karlin, K. D. *J. Am. Chem. Soc.* **2003**, *125*, 16160−16161.

Scheme 6

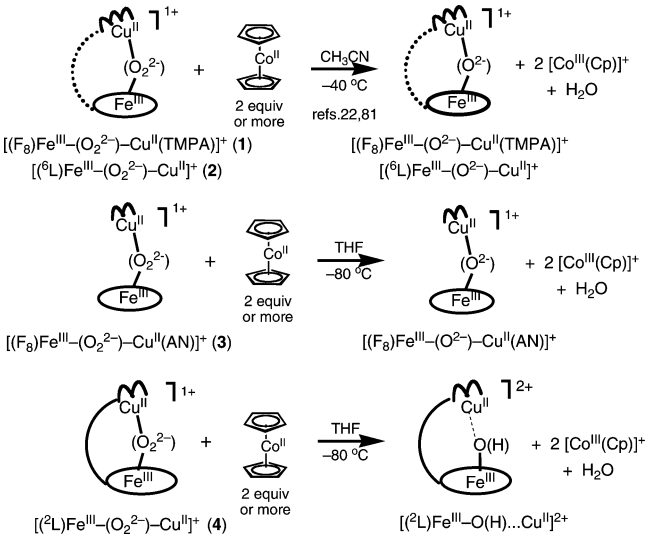

λ_{max} = 262 nm[81] (data not shown).[35,82] In the reaction of [(F_8)Fe^{III}-(O_2^{2-})-Cu^{II}(AN)]$^+$ (**3**) with two or more equivalents of $CoCp_2$, a similar result occurs, Scheme 6; the complete clean conversion to the corresponding oxo-bridged complex [(F_8)Fe^{III}-O-Cu^{II}(AN)]$^+$ takes place in THF at −80 °C, as monitored by UV−vis spectroscopy (Supporting Information, Figures S1 and S17).[83] Reaction of excess $CoCp_2$ with [(^{2}L)-Fe^{III}-(O_2^{2-})-Cu^{II}]$^+$ (**4**) gives a related result (Scheme 6), in that an overall two-electron reduction occurs, giving a mixture of μ-oxo and iron(III) hydroxide complexes within the ^{2}L framework, [(^{2}L)Fe^{III}−O(H)···Cu^{II}]$^{2+}$, based on distinctive UV−vis spectra known for the Fe^{III}−OH and μ-oxo [Fe^{III}−O−Cu^{II}]$^+$ moieties.[65] The ^{2}L binucleating ligand appears not to be well set up to stabilize an Fe^{III}−O−Cu^{II} moiety, and it is very sensitive to solvent water/protons.[23]

Thus, in all cases for peroxo complexes **1**−**4**, reaction even with excess $CoCp_2$ leads only to two-electron reduction chemistry, and either oxo or hydroxo (for **4**) stabilization of iron(III) and Cu(II) precludes further reduction to iron(II) and Cu(I). This contrasts strongly with the results of Collman and co-workers, as mentioned above. A number of factors may be in play. Collman's peroxo complexes are low-spin because of the presence of a tethered axial ligand (pyridyl or imidazolyl) "base" (B, Scheme 5), which is part of the sophisticated superstructured binucleating ligand design, or in certain cases, an excess of an imidazole derivative was added. Thus, the low-spin nature, which would favor reduction to iron(II) (d^6, low-spin) may facilitate the full reduction observed. Another factor could be the likely elongated (by ligand design) Fe···Cu separation in Collman's complexes relative to our series of compounds;[5,35] this would prevent formation of μ-oxo heme−Cu complexes requiring an Fe···Cu separation of ≤3.6 Å.[5] We find pervasive formation of μ-oxo Fe^{III}−O−Cu^{II}(ligand) complexes, that is, from "acid−base" reactions or from thermal transformation products of heme−peroxo−copper(II) compounds.[5] The (porphyrinate)Fe^{III}−O−Cu^{II} entity seems to be a "sink" for heme/Cu/O_2 chemistry in the same way that the μ-oxo (porphyrinate)Fe^{III}−O−Fe^{III}(porphyrinate) compounds are the sink for heme/O_2 chemistry.[8,84,85]

Reactions with *t*-Butyl-Substituted Phenols. Phenol addition to heme−Cu/O_2 adducts is inspired by reactivity observed for the "mixed-valent" C*c*O enzyme form, wherein a tyrosine, as part of a histidine−tyrosine binuclear center cofactor (the His is bound to Cu_B), is thought be a H-atom donor.[5] When either 2,4-*t*Bu_2-phenol or 2,4,6-*t*Bu_3-phenol as good hydrogen atom ($H^+ + e^-$) donors are added to **1**−**4** (Chart 1) solutions at low-temperature, no reactions occur. These conclusions are based on monitoring by UV−vis and EPR (to follow possible phenoxyl radical formation) spectroscopies.

Collman and co-workers[64] recently reported that an exogenously added phenol can be added to a heme−superoxo−copper(I) (i.e., with $Fe^{III}(O_2^-)$···Cu^I moiety), resulting in O−O reductive cleavage; this heme−Cu complex possesses an internal (i.e., appended) imidazole axial base for iron, presumably rendering the system to be low-spin.[88] It is notable that for non-heme iron Fe^{III}−OOR complexes, low-spin rather than high-spin species are amenable to reductive O−O cleavage chemistry as a consequence of weakened peroxide O−O bonds and strengthened Fe−O bonds.[86,87]

Summary and Conclusions

The results described in this paper provide interesting insights into the nature of the peroxo moiety in Fe^{III}−(O_2^{2-})−Cu^{II} complexes **1**−**4** (Chart 1) as revealed by reactivity studies, with CO, PPh_3, acids, cobaltocene, and phenol.

The reactions with *carbon monoxide* and *triphenylphosphine* in part reflect the fact that all of these complexes are in fact dioxygen adducts derived from Fe^{II}/Cu^I/O_2 reactions, since CO or PPh_3 can cause the release of O_2 or its (formal) reduction to the superoxide level now bound to the heme (Schemes 2 and 3). The reversibility/irreversibility of O_2 binding is not the reason for the different CO and PPh_3 reactivity found for the **1**−**4** peroxo complexes because, as was stated at the beginning, the formation of all **1**−**4** peroxo complexes is irreversible. The driving force would appear to be the formation of very stable low-valent Cu^I−CO or Cu^I−PPh_3 fragment, Schemes 2 and 3. In copper−dioxygen chemistry with closely related N_3 tridentate or N_4 tetradentate chelates, the same phenomenon is observed, namely, [LCu^{II}-(O_2^{2-})Cu^{II}L]$^{2+}$ complexes react with either CO or

(82) Scheme 6 indicates water is produced in the reactions of peroxo complexes. While H_2O was not directly detected, our conclusions about the products and stoichiometry of reaction follow from (1) the observation that cobaltocinium cation is formed along with the Fe−oxo−Cu species, suggesting oxide ion would also be a product, and (2), Collman (ref. 35) also suggests an oxide forms in such reactions. We suggest that the two protons would come from solvent water molecules, with the "leftover" hydroxide anions acting as counterions for the 2 equiv of cobaltocinium produced.

(83) The UV−vis features of [(F_8)Fe^{III}-O-Cu^{II}(AN)]$^+$ are shown in Figures S1 and S17; a confirming X-ray structure has been obtained and will be reported elsewhere.

(84) Kurtz, D. M., Jr. *Chem. Rev.* **1990**, *90*, 585−606.
(85) Balch, A. L. *Inorg. Chim. Acta* **1992**, *198*−*200*, 297−307.
(86) Lehnert, N.; Ho, R. Y. N.; Que, L., Jr.; Solomon, E. I. *J. Am. Chem. Soc.* **2001**, *123*, 12802−12816.
(87) Ho, R. Y. N.; Roelfes, G.; Feringa, B. L.; Que, L., Jr. *J. Am. Chem. Soc.* **1999**, *121*, 264−265.

PPh_3 to give 2 LCu^I-L' ($L' = CO$ or PPh_3) + O_2.[28,57−61] Remarkably, one complex does not at all react with CO or PPh_3, $[(F_8)Fe^{III}\text{-}(O_2^{2-})\text{-}Cu^{II}(TMPA)]^+$ (**1**). In summary, there are clear differences in $Fe^{III}-(O_2^{2-})-Cu^{II}$ reactions with CO or PPh_3 that reveal the dioxygen origin of the peroxo group in **2**−**4** and reflect variations in the detailed nature of the peroxo structure and ligand architecture.

The reactions of **1**−**4** with hydrochloric acid lead to good yields of hydrogen peroxide. The procedures used to demonstrate this may be generally useful as a chemical rather than spectroscopic tool to provide evidence that O_2 adducts have a peroxidic nature.[81] The other point is that the chloride present, as an excellent Fe^{III} and Cu^{II} ligand, facilitates release of peroxide and H_2O_2 production. Thus, future use of acids with non-coordinating counteranions (e.g., $H(Et_2O)_2B(C_6F_5)_4$) may lead to the study of interesting and potentially important hydroperoxo heme−copper assemblies.

The reactions of cobaltocene with **1**−**4** are quite different than that observed for heme−copper/O_2 adducts studied by Collman and co-workers. For those, complete reduction to Fe^{II}/Cu^I species occurred, but in our case, only partial reduction occurs; the peroxide is reduced and either Fe^{III}−oxo−Cu^{II} or Fe^{III}−hydroxo···Cu^{II} products form. The origin of the difference most likely lies in the fact that **1**−**4** are high-spin entities not possessing any ligating heme axial "base" (pyridine or imidazole).

These observations are probably also related to our findings on the lack of reactivity of peroxo complexes **1**−**4** even with rather easily oxidizable *t*butyl-substituted phenols. Thus, reductive (protonation) of heme−peroxo−copper complexes would seem to require heme−copper assemblies with axial "base" ligands (*vide supra*), and this is a direction for future in-depth studies of the O−O cleavage process,[88] of broad fundamental interest and of course relevant to C*c*O function.

Experimental Section

Materials and Methods. All reagents and solvents were purchased from commercial sources and were of reagent quality unless otherwise noted. Acetonitrile (CH_3CN) and heptane were distilled from calcium hydride; tetrahydrofuran (THF) was distilled from sodium/benzophenone under argon, and methylene chloride (CH_2Cl_2) was purified over an activated alumina column. Preparation and handling of air-sensitive compounds were performed under an argon atmosphere using standard Schlenk techniques or in a MBraun Labmaster 130 inert atmosphere (<1 ppm O_2, <1 ppm H_2O) glovebox filled with nitrogen. Deoxygenation of solvents was effected either by repeated freeze/pump/thaw cycles or by bubbling with argon for 30−45 min.

Low-temperature UV−vis spectra were recorded on a Hewlett-Packard Model 8453A diode array spectrometer with HP Chemstation software; the instrument was equipped with a variable-temperature Dewar and cuvette assembly as described elsewhere.[53] NMR spectra were measured on a Varian XL-400 NMR instrument at ambient or at low temperatures. All spectra were recorded in 5 mm o.d. NMR tubes, and chemical shifts δ (ppm) were referenced either to an internal standard (Me_4Si) or to residual solvent peaks. Electron paramagnetic resonance (EPR) spectra were obtained in frozen solutions with 4 mm o.d. quartz tubes in a Bruker EMX spectrometer operating at X-band using microwave frequencies around 9.5 GHz, with sample temperature maintained at 77 K. EPR spectra were referenced to 2,2diphenyl-1-picrylhydrazyl (g = 2.0036). IR spectra were obtained at room temperature using a Mattson Galaxy 4030 series FT-IR spectrophotometer. Mass spectrometry (ESI in the positive ion mode) was measured on a Thermo-Finnigan LCQ Deca.

Syntheses. The reduced complexes $(F_8)Fe^{II}\cdot H_2O$,[38,89] $[Cu^I(TMPA)(CH_3CN)](ClO_4)$,[61] $[Cu^I(AN)](B(C_6F_5)_4)$,[39] $[(^6L)Fe^{II}\cdots Cu^I](B(C_6F_5)_4)$,[21] and $[(^2L)Fe^{II}\cdots Cu^I](B(C_6F_5)_4)$[23] were synthesized according to published procedures.

Generation of $[(F_8)Fe^{III}\text{-}(O_2^{2-})\text{-}Cu^{II}(AN)]^+$ (3) and Thermal Decomposition. Equimolar amounts of $(F_8)Fe^{II}\cdot H_2O$ and $[Cu^I(AN)](B(C_6F_5)_4)$ were dissolved in 10 mL deoxygenated THF in glovebox and transferred to a modified low-temperature cuvette assembly equipped with a Schlenk-type sidearm.[53] After the mixture was cooled to 193 K, UV−vis spectra of the reduced mixture were taken [λ_{max} = 422 (Soret), 542 nm, see Figure 1]. Then, generation of the peroxo adduct **3** [λ_{max} = 418 (Soret), 478, 538, and 561 nm] was accomplished by bubbling dioxygen through the solution. Complex **3** underwent thermal decomposition (with 1/2 mole of O_2 liberated from each mole of **3**, determined spectrophotometrically using a pyrogallol solution) to the corresponding μ-oxo complex $[(F_8)Fe^{III}\text{-}O\text{-}Cu^{II}(AN)]^+$ with the characteristic red-shifted Soret band at 440 nm and broad 557 nm absorption (Figure S1). This disproportionation chemistry is observed with the other heme−peroxo−copper complexes **1** and **2**, and perspectives on these interesting transformations are discussed elsewhere.[4,17,21] This μ-oxo product is thermally stable, but in presence of moisture, it decomposes to the corresponding μ-hydroxo $[(F_8)Fe^{III}\text{-}(OH^-)\text{-}Cu^{II}\text{-}(AN)]^{2+}$, with absorptions at 410 and 572 nm.

Resonance Raman Studies on $[(F_8)Fe^{III}\text{-}(O_2^{2-})\text{-}Cu^{II}(AN)]^+$ (3). In the glovebox, 5 mM solutions of an equimolar mixture of $(F_8)\text{-}Fe^{II}\cdot H_2O$ and $[(AN)Cu^I]^+$ in THF were prepared and transferred to NMR tubes (~0.5 mL solution in each tube) and capped with tight-fitting septa. The sample tubes were placed in a cold bath (dry ice/acetone) for ~15 min and oxygenated using $^{16}O_2$ and $^{18}O_2$ ($^{18}O_2$ gas was purchased from ICON, Summit, NJ, and $^{16}O_2$ gas was purchased from BOC gases, Murray Hill, NJ). The labeled gases were cooled in dry ice for 5 min and injected through the solution by using a Hamilton gastight syringe. The oxygenated samples were set in a cold bath for 10 min, after which the sample tubes were frozen in liquid N_2 and sealed by flame. Resonance Raman spectra were collected on a McPherson 2061/ 207 spectrograph in a 0.67 m configuration equipped with a Kaiser Optical supernotch filter to minimize interferences from the Rayleigh scattering. Raman scattered light, gathered in a backscattering geometry, was dispersed using a 2400 gr/mm holographic grating and analyzed using a liquid nitrogen-cooled Princeton Instruments LN-1100PB CCD detector. A Coherent Innova 302 krypton ion laser was used as the source for the 413 nm excitation. The samples were placed in a custom glass Dewar equipped with a copper coldfinger cooled with liquid nitrogen to maintain the sample temperature at ~90 K. A custom sample spinning was employed to minimize sample degradation upon laser illumination. Additionally, the laser power was kept below 10 mW, and individual spectra were compared to confirm the integrity of the samples during the data acquisition. Vibration

(88) We have also described related chemistry. While **3** does not react with 2,4,-*t*Bu$_2$-phenol, if dicylohexylimidazole is first added to form a low-spin adduct, this then reacts with the phenol to give O-O cleavage and a (porphryinate)Fe^{IV}=O (ferryl) product, plus the bis-phenol 3,3′,5,5′-tetra-tert-butyl-2,2′-dihydroxybiphenyl. Details will be reported elsewhere.

(89) Kopf, M.-A.; Neuhold, Y.-M.; Zuberbühler, A. D.; Karlin, K. D. *Inorg. Chem.* **1999**, *38*, 3093−3102.

frequencies were calibrated relative to an internal standard and are accurate to ± 1 cm^{-1}.

Generation of $[(F_8)Fe^{III}\text{-}(O_2^{2-})\text{-}Cu^{II}(TMPA)]^+$ (1) for Reactions Monitored by UV−vis Spectroscopy. In a typical experiment, a stock solution of equimolar amounts of $(F_8)Fe^{II}\cdot H_2O$ (20 mg) and $[Cu^{I}(TMPA)(CH_3CN)](ClO_4)$ (12 mg) in 19.1 mL of deoxygenated CH_3CN (15 g) was prepared in glovebox. Then, 4.1 mL (3.20 g) of stock solution was diluted to 12.7 mL (10 g) and transferred to a modified low-temperature cuvette assembly equipped with a Schlenk-type sidearm.[53] After the mixture was cooled to 233 K, generation of the peroxo adduct **1** was carried out by bubbling the chilled solution with dioxygen. Removal of excess O_2 was performed by application of 3−5 vacuum/Ar cycles.

Generation of $[(^6L)Fe^{III}\text{-}(O_2^{2-})\text{-}Cu^{II}]^+$ (2) for Reactions Monitored by UV−vis Spectroscopy. In a typical experiment, 9 mg of $[(^6L)Fe^{II}\cdots Cu^{I}][B(C_6F_5)_4]$ was dissolved in ∼20 g of deoxygenated CH_3CN, THF, or acetone in a glovebox and transferred to a modified low-temperature cuvette assembly equipped with a Schlenk-type sidearm.[53] After the mixture was cooled to 233 or 193 K (depending of the solvent), generation of the peroxo adduct **2** was carried out by bubbling the chilled solution with dioxygen. Removal of excess O_2 is performed by application of 3−5 vacuum/Ar cycles.

Generation of $[(F_8)Fe^{III}\text{-}(O_2^{2-})\text{-}Cu^{II}(AN)]^+$ (3) and $[(^2L)Fe^{III}\text{-}(O_2^{2-})\text{-}Cu^{II}]^+$ (4) for Reactions Monitored by UV−vis Spectroscopy. Complexes **3** and **4** were generated in a similar way to that described for **1** and **2**, respectively (see above).

Reaction of $[(^6L)Fe^{III}\text{-}(O_2^{2-})\text{-}Cu^{II}]^+$ (2) with CO. (a) UV−vis Analysis. The peroxo compound **2** was generated in situ in CH_3CN at −40 °C as described above, and its UV−vis spectrum was recorded. CO was bubbled through the solution for ∼10 s, using a long needle, and then the UV−vis spectrum of the product was taken. The product of the reaction, $[(^6L)Fe^{II}-CO\cdots Cu^{I}\text{-}CO]^+$, was proven to be stable at room temperature.

(b) IR Analysis of the Product. After the UV−vis experiment (see above), an aliquot of the solution at room temperature was transferred to a SPECAC cell and its IR spectrum was recorded (see Figure 3 and S2).

Reaction of $[(F_8)Fe^{III}\text{-}(O_2^{2-})\text{-}Cu^{II}(AN)]^+$ (3) with CO. (a) UV−vis Analysis. The peroxo compound **3** was generated in situ in THF at −80 °C as described above, and its UV−vis spectrum was recorded (Figure S3). CO was bubbled through the solution for ∼10 s, and then the UV−vis spectrum of the product was taken. At least one of the products of the reaction, $(F_8)Fe^{II}-CO$ (which dominates the UV−vis features of the spectrum) proved to be stable at room temperature.

(b) IR Analysis of the Product. After the UV−vis experiment, an aliquot of the solution at room temperature was transferred to a SPECAC cell, and its IR spectrum was recorded (see Figure S4).

Investigations on $[(F_8)Fe^{III}\text{-}(O_2^{2-})\text{-}Cu^{II}(TMPA)]^+$ (1) with PPh_3. In a UV−vis cuvette assembly, 10.2 mL (8 g) of a 0.4 mM solution of $[(F_8)Fe^{III}\text{-}(O_2^{2-})\text{-}Cu^{II}(TMPA)]^+$ (**1**) was generated in CH_3CN at −40 °C ; then 5 equiv of PPh_3 was added (176 μL of a 115 mM fresh stock solution prepared with 150.5 mg of PPh_3 in 5 mL of acetonitrile). The cuvette was kept in a freezer at −32 °C (with another cuvette containing only the peroxo compound **1** as a control), and there was no change in the original UV−vis spectrum of the peroxo compound **1** for at least 5 days. Furthermore, the oxidation of PPh_3 was tested by ^{31}P NMR spectroscopy, and the result was negative, confirming that the peroxo compound **1** is stable before PPh_3.

Reaction of $[(F_8)Fe^{III}\text{-}(O_2^{2-})\text{-}Cu^{II}(AN)]^+$ (3) with PPh_3. In a UV−vis cuvette assembly, a solution of $[(F_8)Fe^{III}\text{-}(O_2^{2-})\text{-}Cu^{II}(AN)]^+$ (**3**) was generated in THF at −80 °C as described above; a concentrated THF solution containing 5 equiv of PPh_3 (prepared as described above) was then added. The UV−vis spectra of the original peroxo complex **3** and the product of the reaction were recorded (Figure 4). In a separate experiment, the oxidation of PPh_3 was investigated by ^{31}P NMR spectroscopy. The low-temperature reaction was carried out in a Schlenk flask and then, at room temperature, the solvent was removed, and the solid residue was taken with acetone-d_6. The ^{31}P NMR spectrum show no significant peak for $O{=}PPh_3$.

Reaction of $[(F_8)Fe^{III}\text{-}(O_2^{2-})\text{-}Cu^{II}(TMPA)]^+$ (1) with HCl. (a) UV−vis Analysis in CH_3CN. The peroxo compound **1** was generated in situ in CH_3CN at −40 °C as described above, and then 0.5, 1.0, 1.5, and 2.0 equiv of HCl (50, 100, 150, and 200 μL, respectively, of HCl stock solution prepared with 100 mg of a hydrogen chloride 1.0 M solution in diethyl ether, Aldrich, in 10 mL of CH_3CN) were added, and the respective spectra recorded at − 40 °C (see Figure 5). Finally excess HCl was added, but there was no further change in the UV−vis spectrum.

(b) UV−vis Analysis in CH_2Cl_2. Fifteen milligrams of solid **1** (isolated as reported in ref 19) was dissolved in 25 mL of precooled CH_2Cl_2 (0.46 mM), and 7 mL of that solution was transferred to a cuvette assembly with sidearm stopcock. One and two equivalents of HCl (50 and 100 μL, respectively, of HCl stock solution prepared with 472 mg hydrogen chloride 1.0 M solution in diethyl ether, Aldrich, in 10 mL CH_2Cl_2) were added, and the respective spectra were recorded at −80 °C (see Figure S5). Finally, the solution was warmed to RT, and then the spectrum of the decomposition product was recorded at −80 °C.

(c) ^1H NMR Analysis in CD_3CN. In the glovebox, 20 mg of $(F_8)Fe^{II}\cdot H_2O$ and 12 mg of $[Cu^{I}(TMPA)(CH_3CN)]ClO_4$ were dissolved in 5 mL of deoxygenated CD_3CN (4.9 mM), and the mixture was transferred to a Schlenk flask capped with a septum. Outside the glovebox, the solution was cooled to −40 °C and bubbled with dioxygen to generate the peroxo compound **1**. Then 0.6 mL of the solution (containing 0.0029 mmol of **1**) was transferred to a screw-capped NMR tube, and the ^1H NMR spectrum was recorded at −40 °C. One equivalent of HCl (50 μL, 0.0029 mmol, CH_3CN solution prepared from diethyl ether 1.0 M solution of hydrogen chloride, Aldrich) was then introduced via syringe; the solution was shaked quickly, and the ^1H NMR spectrum was recorded at −40 °C. This process of adding 1 equiv of HCl and recording spectrum was repeated to complete the reaction.

(d) EPR Analysis in CH_3CN. In the glovebox, 20 mg of $(F_8)Fe^{II}\cdot H_2O$ and 12 mg of $[Cu^{I}(TMPA)(CH_3CN)]ClO_4$ were dissolved in 10.2 mL (8 g) of CH_3CN, and the mixture was transferred to a 25 mL Schlenk flask equipped with a stir-bar and capped with a septum. Outside the glovebox, the solution was cooled to −40 °C and bubbled with dioxygen to generate the peroxo compound **1**. Then, 0.30 mL of the solution was transferred to an EPR tube and the EPR spectrum was recorded at 77 K (conc ∼2 mM). One equivalent of HCl (48.5 μL 1.0 M diethyl ether solution of hydrogen chloride, Aldrich) was then added to the mother solution, and a new aliquot of 0.30 mL was taken; then, the EPR spectrum was recorded at 77 K. This process of adding 1 equiv of HCl and recording spectrum was repeated to complete the reaction.

(e) Quantitative Determination of H_2O_2 by the Peroxotitanyl Method. Equimolar amounts of $(F_8)Fe^{II}\cdot H_2O$ (24.9 mg) and $[Cu^{I}(TMPA)(CH_3CN)]ClO_4$ (14.8 mg) were dissolved in 10 mL of CH_3CN (conc = 3 mM) in the glovebox. The solution was brought out of the glovebox and immersed in a cold bath at − 40 °C, and dioxygen was then bubbled through the solution to generate the peroxo compound **1**. Excess O_2 was removed by several vacuum/Ar cycles; then 10 equiv of HCl (0.3 mL of 1.0 M diethyl ether solution of hydrogen chloride, Aldrich) was added, and the dark red solution turned to dark green. The solution was removed from the cold bath, followed by addition of 20 mL of distilled water

(final volume = 30.3 mL). A suspension is formed because of the insolubility of $(F_8)Fe^{III}-Cl$ in the solvent mixture. H_2O_2 was determined spectrophotometrically (at 408 nm) upon addition of 1 mL of titanyl reagent (titanium(IV) oxysulfate in sulfuric acid, Riedel de Haën) to a 10 mL suspension, followed by centrifugation. A calibration curve was made in the same solvent mixture of the reaction (CH_3CN/Ether/H_2O). The yield of H_2O_2 was determined to be 70% on the basis of two experiments.

Reaction of $[(F_8)Fe^{III}\text{-}(O_2^{2-})\text{-}Cu^{II}(TMPA)]^+$ (1) with HOTf (triflic acid), HBF_4, $[H(Et_2O)_2][B(C_6F_5)_4]$, and $[(CH_3)_3O](BF_4)$ (Trimethyloxonium Tetrafluoroborate). The peroxo compound **1** was generated in situ in CH_3CN at −40 °C as described above; then HOTf (trifluoromethanesulfonic acid) in different amounts (from an acetonitrile stock solution prepared form a previously distilled acid, Aldrich ampule) were added with syringe, and the respective spectra were recorded at −40 °C (see Figure S9). Finally excess acid was added but there was no further change in the UV−vis spectrum. In the same manner, the experiments with HBF_4 (using an acetonitrile stock solution prepared form Aldrich reagent) (Figure 8), $[H(Et_2O)_2][B(C_6F_5)_4]$ (acetonitrile solution of the acid prepared following a modified procedure of that published by P. Jutzi et al.)[79] (Figure S13), and $[(CH_3)_3O](BF_4)$ (acetonitrile solution prepared from Aldrich reagent) were carried out.

Reaction of $[(^6L)Fe^{III}\text{-}(O_2^{2-})\text{-}Cu^{II}]^+$ (2) with HCl. (a) UV−vis Analysis in Acetone. The peroxo compound **2** was generated in situ in acetone at −80 °C as described above; then 2 equiv and excess HCl (taken from hydrogen chloride 1.0 M solution in diethyl ether, Aldrich) were added, and the respective spectra were recorded at −40 °C (see Figure S14).

(b) Analysis of Residue by ^{1}H NMR. After the reaction was UV−vis monitored (see above), the solvent was removed by vacuum, and the solid residue taken with acetone-d_6. ^{1}H NMR spectrum of the residue showed the paramagnetic pyrrole signal at 85 ppm, characteristic of $[(^6L)Fe^{III}-Cl\cdots Cu^{II}-Cl]^+$.

(c) Quantitative Determination of H_2O_2 by the Peroxotitanyl Method. The yield of H_2O_2 (80%) generated upon acidification of **2** was determined in a similar manner to that described for **1** (see above).

Reaction of $[(F_8)Fe^{III}\text{-}(O_2^{2-})\text{-}Cu^{II}(AN)]^+$ (3) with HCl. (a) UV−vis Analysis. The peroxo compound **3** was generated in situ in THF at −80 °C as described above; then 1, 2, and 4 equiv of HCl (taken from hydrogen chloride 1.0 M solution in diethyl ether, Aldrich) were added, and the respective spectra were recorded at −80 °C (see Figure S15).

(b) Analysis of Residue by ^{1}H NMR. After the reaction had been UV−vis monitored (see above), the solvent was removed by vacuum, and the solid residue taken with chloroform-*d*. ^{1}H NMR spectrum of the residue showed the paramagnetic pyrrole signal at 82 ppm, characteristic for $(F_8)Fe^{III}-Cl$.

(c) Quantitative Determination of H_2O_2 by the Peroxotitanyl Method. The yield of H_2O_2 (77%) generated upon acidification of **3** was determined in a similar manner to that described for **1** (see above).

Reaction of $[(^2L)Fe^{III}\text{-}(O_2^{2-})\text{-}Cu^{II}]^+$ (4) with HCl. (a) UV−vis Analysis. The peroxo compound **4** was generated in situ in THF at −80 °C as described above (at Soret band scale); then 1, 2, and excess equiv of HCl (taken from hydrogen chloride 1.0 M solution in diethyl ether, Aldrich) were added, and the respective spectra were recorded at −80 °C (see Figure S16).

Reaction of $[(F_8)Fe^{III}\text{-}(O_2^{2-})\text{-}Cu^{II}(AN)]^+$ (3) with $CoCp_2$ by UV−vis Spectroscopy. To a solution of **3** generated as described above [λ_{max} = 477(sh), 538, 561(sh) nm; THF, 193 K] (see Figure S17) was added a THF solution of $CoCp_2$ in small aliquots. The addition of cobaltocene produced an immediate change in the UV−vis spectrum corresponding to a loss of the peroxo complex **3** and formation of the oxo product $[(F_8)Fe^{III}\text{-O-}Cu^{II}(AN)]^+$ [λ_{max} = 557 nm]. Full formation of the oxo product was achieved after the addition of 2 equiv of $CoCp_2$, while excess $CoCp_2$ did not produce any further change in the UV−vis spectrum.

Reaction of $[(^2L)Fe^{III}\text{-}(O_2^{2-})\text{-}Cu^{II}]^+$ (4) with $CoCp_2$ by UV−vis Spectroscopy. The reaction was carried out in the same manner as that for complex **3** (see above).

Acknowledgment. We thank the National Institutes of Health (GM60353, K.D.K.; GM34468, T. M. Loehr and P.M-L.) and Universidad Nacional de San Luis-Argentina (E.E.C) for research support.

Supporting Information Available: UV−vis spectrum of μ-oxo complex $[(F_8)Fe^{III}\text{-O-}Cu^{II}(AN)]^+$ (Figure S1), IR spectrum of $[(^6L)Fe^{II}-CO\cdots Cu^{I}-CO]^+$ (Figure S2), UV−vis spectra monitoring the reaction of $[(F_8)Fe^{III}\text{-}(O_2^{2-})\text{-}Cu^{II}(AN)]^+$ (**3**) with CO (Figure S3), IR spectrum of the products $[(THF)(F_8)Fe^{II}(CO)]$ and $[(AN)Cu^{I}-CO]^+$ generated upon CO reaction of peroxo complex **3** (Figure S4), IR spectrum of authentic $[(AN)Cu^{I}-CO]^+$ (Figure S5), small distortion at the EPR upfield copper(II) signal of $[Cu^{II}(TMPA)Cl]^+$ upon addition of excess HCl (Figure S6), Positive ion electrospray (ESI) mass spectrum of the reaction product of $[(F_8)Fe^{III}\text{-}(O_2^{2-})\text{-}Cu^{II}(TMPA)]^+$ (**1**) with 2 equiv of HCl in CH_3CN at −40 °C with calculated positive ESI mass spectrum of the cation $[Cu^{II}(TMPA)Cl]^+$ (Figure S7), UV−vis spectra for the reaction of $[(F_8)Fe^{III}\text{-}(O_2^{2-})\text{-}Cu^{II}(TMPA)]^+$ (**1**) with HCl in CH_2Cl_2 (Figure S8), UV−vis spectra for the reaction of $[(F_8)Fe^{III}\text{-}(O_2^{2-})\text{-}Cu^{II}(TMPA)]^+$ (**1**) with triflic acid (HOTf) (Figure S9), positive ion electrospray (ESI) mass spectrum of the reaction product of $[(F_8)Fe^{III}\text{-}(O_2^{2-})\text{-}Cu^{II}(TMPA)]^+$ (**1**) with 2 equiv of triflic acid (HOTf) in CH_3CN at −40 °C with calculated positive ESI mass spectrum of the cation $[Cu^{II}(TMPA)CN]^+$ (Figure S10), X-band EPR spectrum of the reaction product of $[(F_8)Fe^{III}\text{-}(O_2^{2-})\text{-}Cu^{II}(TMPA)]^+$ (**1**) with 2 equiv of HBF_4 in CH_3CN at −40 °C (Figure S11), positive ion electrospray (ESI) mass spectrum of the reaction product of $[(F_8)Fe^{III}\text{-}(O_2^{2-})\text{-}Cu^{II}(TMPA)]^+$ (**1**) with 2 equiv of HBF_4 in CH_3CN at −40 °C (Figure S12), UV−vis spectra for the reaction of $[(F_8)Fe^{III}\text{-}(O_2^{2-})\text{-}Cu^{II}(TMPA)]^+$ (**1**) with 1 equiv of $[H(Et_2O)_2][B(C_6F_5)_4]$ and for the reaction of $[(F_8)Fe^{III}\text{-}(O_2^{2-})\text{-}Cu^{II}(TMPA)]^+$ (**1**) with 1 equiv of $(CH_3)_3OBF_4$ (Figure S13), UV−vis spectra for the reaction of $[(^6L)Fe^{III}\text{-}(O_2^{2-})\text{-}Cu^{II}]^+$ (**2**) with HCl (Figure S14), UV−vis spectra for the reaction of $[(F_8)Fe^{III}\text{-}(O_2^{2-})\text{-}Cu^{II}(AN)]^+$ (**3**) with HCl (Figure S15), UV−vis spectra for the reaction of $[(^2L)Fe^{III}\text{-}(O_2^{2-})\text{-}Cu^{II}]^+$ (**4**) with HCl (Figure S16), and reduction of $[(F_8)Fe^{III}\text{-}(O_2^{2-})\text{-}Cu^{II}(AN)]^+$ (**3**) to $[(F_8)Fe^{III}\text{-O-}Cu^{II}(AN)]^+$ by addition of 2 equiv of cobaltocene monitored by UV−vis spectroscopy (Figure S17). This material is available free of charge via the Internet at http://pubs.acs.org.

IC700363K